Research Article Open Access

Fuzhen Pang*, Haichao Li*, Xuhong Miao, and Xueren Wang

A modified Fourier solution for vibration analysis of moderately thick laminated annular sector plates with general boundary conditions, internal radial line and circumferential arc supports

DOI 10.1515/cls-2017-0014
Received Jan 02, 2017; accepted Apr 07, 2017

Abstract: In this paper, a modified Fourier solution based on the first-order shear deformation theory is developed for the free vibration problem of moderately thick composite laminated annular sector plates with general boundary conditions, internal radial line and circumferential arc supports. In this solution approach, regardless of boundary conditions, the displacement and rotation components of the sector plate are written in the form of the trigonometric series expansion in which several auxiliary terms are added to ensure and accelerate the convergence of the series. Each of the unknown coefficients is taken as the generalized coordinate and determined using the Raleigh-Ritz method. The accuracy and reliability of the present solution are validated by the comparison with the results found in the literature, and numerous new results for composite laminated annular sector plates considering various kinds of boundary conditions are presented. Comprehensive studies on the effects of elastic restraint parameters, layout schemes and locations of line/arc supports are also made. New results are obtained for laminated annular sector plates subjected to elastic boundary restraints and arbitrary internal radial line and circumferential arc supports in both directions, and they may serve as benchmark solutions for future researches.

Keywords: Free vibration; General boundary conditions; Laminated annular sector plates; Internal radial line supports; Internal circumferential arc supports; Modified Fourier series; Arbitrary lamination schemes

1 Introduction

As one of the important structural components, composite laminated annular sector plates have found wide applications as structural members in aerospace, marine and other industries. Notably, these plates frequently work in complex environments and may suffer to arbitrary boundary restraints. In addition, intermediate line/arc supports may be placed to reduce the magnitude of dynamic stresses, static stresses and plate displacements as well as satisfy special functional requirements. Therefore a thorough understanding of the vibration behaviors of composite laminated annular sector plates with general boundary restraints and internal radial line and circumferential arc supports is of great interest for the designers to realize proper and comparatively accurate design of machines and structures.

To deal with the vibration of composite laminated annular sector plates, the plate theory and computational approach, which are two powerful tools, need mastering first. So far, huge amounts of research efforts have been devoted to vibration analysis and dynamic behavior study of plates and an enormous variety of plate theories and computational methods have been proposed and developed. As for the plate deformation theory, a significant number of two-dimensional (2-D) theory and three-dimensional (3-D) elasticity theory are given in previous studies. The commonly used 2-D theories contains the classical plate theory (CPT), the first-order shear deformation theory (FSDT), and the higher-order shear deformation theory (HSDT). More detailed information about the progress of this subject can be found in the monographs respectively by Leissa [1], Qatu [2], Reddy [3], and Carrera [4]. The CPT [5–10] was firstly employed to study various characteristics of thin

***Corresponding Author: Fuzhen Pang:** College of Shipbuilding Engineering, Harbin Engineering University, Harbin, 150001, PR China; Naval Academy of Armament, Beijing, 100161, PR China; Email: pangfuzhen@hrbeu.edu.cn; Tel. +86-451-82519161
***Corresponding Author: Haichao Li:** College of Shipbuilding Engineering, Harbin Engineering University, Harbin, 150001, PR China; Email: lihaichao@hrbeu.edu.cn; Tel.: +86-451-82519161

Xuhong Miao, Xueren Wang: Naval Academy of Armament, Beijing, 100161, PR China

plates. In view of the fact that CPT ignores the effect of shear deformation through the thickness, it's only suitable for thin plate structures and deserves proper results at low frequency. To eliminate this deficiency, the FSDT was developed then, which assumes constant states of the transverse shear stresses through the plate thickness. There is also a great deal of research on the plate structure on the basis of FSDTs [11–23]. Generally, the shear correction factor is used to adjust the transverse shear stiffness as a constant, which differs from the fact that the shear correction factor is determined by the material properties and boundary conditions. Therefore, a theory considering the effects of both shear and normal deformations is developed, which is called HSDTs. In the HSDTs, the shear correction factor is no longer used. Various HSDTs are proposed in literature [24–26]. Compared with 2-D theories, the 3-D elasticity theory gets rid of all hypotheses, so it can not only provide realistic results but also bring out physical insights. The investigations based on 3-D elasticity theory can be seen in Ref. [27–32]. However, the HSDTs and 3-D elasticity theory introduce mathematical and computational complexities and require more computational demanding compared with those FSDTs. Seeing from the existing literature, we can know that with proper shear correction factor, the first-order shear deformation theory is adequate enough to predict the vibration behaviors of moderately thick plates. In view of this, the first-order shear deformation shell theory is just adopted to formulate the theoretical model in the present work.

Then, let's turn our eye to the computational model of composite laminated annular sector plates, which is the other important tool for us to have a good understanding of structural behaviors. Similarly, huge amounts of analytical and numerical methods for studying the vibration of composite laminated annular sector plates have been proposed and developed. Salehi and Sobhani [17] used the dynamic relaxation numerical method and the finite difference discretization technique for geometrically linear and non-linear elastic analyses of thick composite sector plates. Sharma *et al.* [18] presented a simple analytical formulation to deal with the eigenvalue problem of buckling and free vibration analysis of shear deformable laminated sector plates which are made up of cylindrically orthotropic layers. Houmat [19] performed large amplitude free vibration of shear deformable laminated composite annular sector plates for clamped boundary condition by finite element method. Andakhshideh *et al.* [20] extended the generalized differential quadrature method for nonlinear static analysis of laminated sector plates with any combination of clamped, simply supported and free edges. Maleki and Tahani [21] employed the generalized differential quadrature method to study the bending of laminated sector plates with both polar and rectilinear orthotropy. Golmakani and Mehrabian [22] performed the elastic large deflection analysis of axisymmetric ring-stiffened circular and annular general angle-ply laminated plates subjected to transverse uniform load by dynamic relaxation (DR) method. Sharma [23] investigated the free vibration of laminated sector plates with elastic edges by using differential quadrature method. Srinivasanal and Thiruvenkatachari [28] presented an integral equation technique for free vibration analysis of laminated annular sector plates with clamped boundary condition. Ding and Xu [29] using the finite Hankel transform to study the axisymmetric vibration of laminated f laminated annular plates composed of transversely isotropic layers. Xu [30] presented a new state space formulations for the free vibration of circular, annular and sectorial plates are established by introducing two displacement functions and two stress functions. Malekzadeh *et al.* [31] used differential quadrature method to analyze the free vibration analysis of thick laminated annular sector plates with simply supported radial edges and arbitrary boundary conditions on their circular edges. Lately, Malekzadeh *et al.* [32] employed a three-dimensional hybrid method to study the dynamic response of thick laminated annular sector plates with simply supported radial edges and a radially distributed line load. Fantuzzi *et al.* [33] employed strong form finite elements to conduct the free vibration study of laminated arbitrarily shaped plates including a quarter of an elliptic plate, a parabolic plate and an annular sector plate.

From the above review, it's not hard to see that each method and technique can be only applied to a particular type of classical boundary conditions, *i.e.*, simply-supported supports, clamped boundaries and free edges. In such case, constant modifications of the solution procedures and corresponding computation codes are required to deal with different boundary conditions. And it could also become a very tedious work and result in repetitive programming and a huge computational cost because the boundary conditions of a laminated annular sector plates cannot always be classical in practical engineering applications. A variety of possible boundary restraining cases, including classical boundary conditions, elastic restraints and their combinations may be encountered in the engineering practices. However, to the best of the authors' knowledge, the free vibration characteristics of the composite laminated annular sector plates with general boundary conditions, internal radial line and circumferential supports have not been investigated yet. Therefore, it is necessary and of great significance to develop a unified, efficient and accurate formulation which is capable

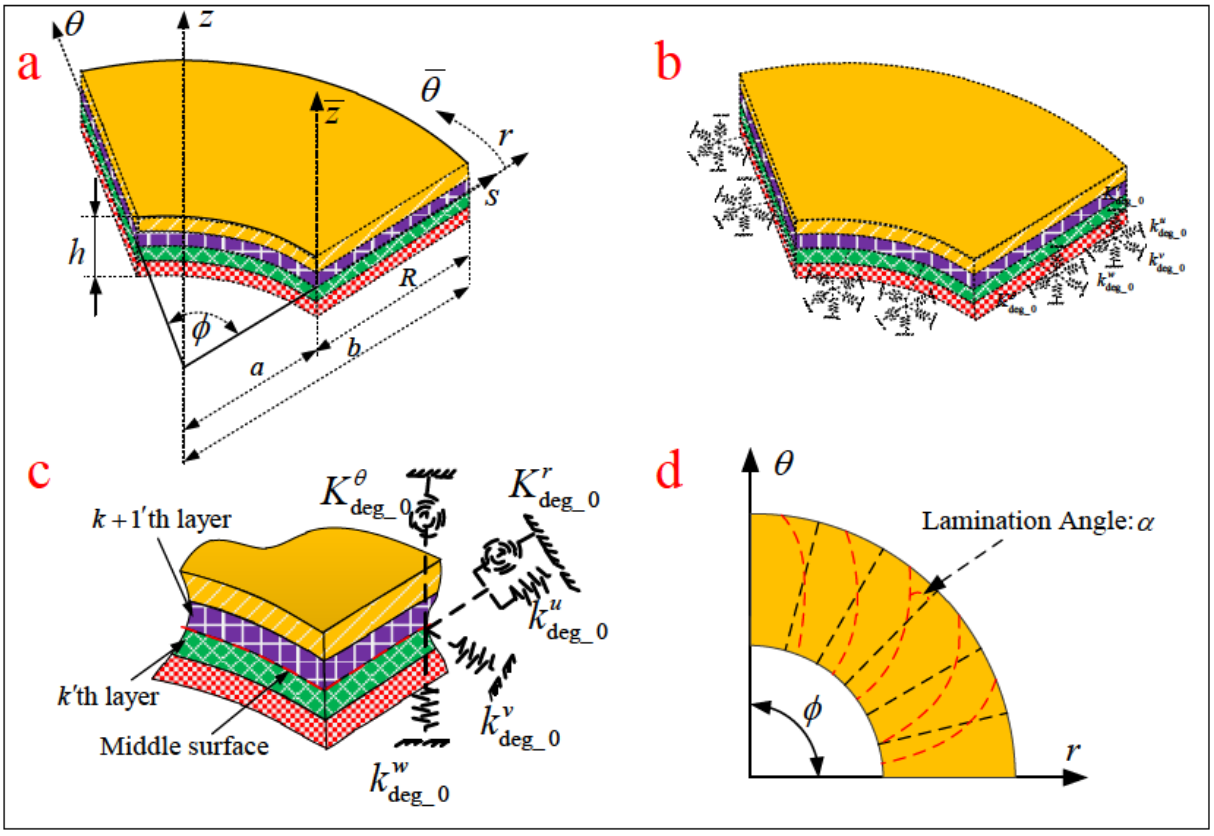

Figure 1: Schematic diagram of a moderately thick composite annular sector plate with elastically restrained edges: (a) geometry and dimensions; (b) partial boundary spring; (c) partial view; (d) lamination angle.

of universally dealing with composite laminated annular sector plates with general boundary conditions, internal radial line and circumferential supports.

Recently, a modified Fourier series technique proposed by Li [34, 35] is widely used in the vibrations of plates and shells with general boundary conditions by Ritz method, *e.g.*, [36–67]. Therefore, the present work can be considered as an extension of the method and attempts to provide a unified solution method for the free vibrations of composite laminated annular sector with general boundary conditions, internal radial line and circumferential supports. Concretely, to derive the theoretical formulation, in addition to the modified Fourier series method, the Ritz procedure and the artificial spring boundary technique are also introduced. The artificial spring boundary condition is adopted to simulate the general boundary condition and the Hamilton's principle based on the first-order shear deformation theory is used to derive the motion equation and related boundary equations. Each component of displacements and rotations of those structures, regardless of the form of the plates and boundary conditions, is expressed as a modified Fourier series, which is constructed as the linear superposition of a standard Fourier cosine series supplemented with auxiliary polynomial functions. The auxiliary polynomial functions are introduced to eliminate all the relevant discontinuities with the displacement and its derivatives at the edges and to accelerate the convergence of series representations. The accuracy and reliability of the current solutions are confirmed by comparing the present results with those available in the literature, and numerous new results for composite laminated annular sector with elastic boundary restraints, internal radial line and circumferential supports are presented. The effects of the elastic restraint parameters, layout schemes, number of lamina and locations of line/arc supports are also studied and reported.

2 Theoretical formulations

2.1 Description of the model

Figure 1 shows a laminated annular sector plate with thickness h, inner radius a, outer radius b, width R of plate in the radial direction and sector angle ϕ. The geometry and

dimensions are defined in an orthogonal cylindrical coordinate system (r, θ, z). A local coordinate system s, θ, z is also shown in the Fig. 1(a), which will be used in the analysis. Since the main focus of this paper is to develop a modified Fourier solution for the vibration analysis of composite laminated annular sector plates with general boundary conditions, thus, in order to satisfy the request, the artificial spring boundary technique [49, 50, 62, 68] is adopted here (seen in Fig. 1(b)), in which three groups of linear springs (k_u, k_v, k_w) and two group of rotational springs (K_R, K_θ) are restrained at every edge of the plate to simulate the given boundary conditions. The stiffness values of these boundary springs can be selected from zero to infinity, and through this operation, different boundary forces can be simulated and imposed on the mid-plane of plate. For instance, when the spring stiffness is set substantially larger than the plate bending rigidity, the clamped boundary condition (C) is essentially realized. Specifically, k_ξ^u, k_ξ^v, k_ξ^w, K_ξ^R and K_ξ^θ (ξ=deg_0, deg_1, r_0 and r_1) are used to indicate the rigidities (per unit length) of the boundary springs at the boundary $\theta = 0$, $\theta = \phi$, $s = 0$ and $s = R$, respectively, see Fig. 1(b-c).

For the sake of brevity, the layers of the laminated plates are made from the same composite material and of equal thickness. The included angle between the material coordinate of the k'th layer and the r-axis of the plate is denoted by α, and Z^k and Z^{k+1} indicate the distances from the undersurface and the top surface of this layer to the referenced plane (as shown in Fig. 1(c-d)).

2.2 Kinematic relations and stress-strain relations

The assumed displacement field for the composite laminated annular sector plates based on first-order shear deformation plate theory can be written as follows:

$$\overline{u}(r, \theta, z, t) = u_0(r, \theta, t) + z\psi_r(r, \theta, t) \tag{1a}$$

$$\overline{v}(r, \theta, z, t) = v_0(r, \theta, t) + z\psi_\theta(r, \theta, t) \tag{1b}$$

$$\overline{w}(r, \theta, z, t) = w_0(r, \theta, t) \tag{1c}$$

where u_0, v_0 and w_0 denote the displacements of corresponding point on reference surface in the r, θ and z directions, respectively. ψ_r and ψ_θ are the rotations of normal to the reference surface about the r and θ direction, respectively, and t is the time. According to the assumption of small deformation and the linear strain–displacement relation, the strain components of functionally graded circular, annular and sector plates can be written as below:

$$\varepsilon_r = \varepsilon_r^0 + z\kappa_r, \quad \varepsilon_\theta = \varepsilon_\theta^0 + z\kappa_\theta \tag{2a}$$

$$\gamma_{r\theta} = \gamma_{r\theta}^0 + z\kappa_{r\theta}, \quad \gamma_{rz} = \gamma_{rz}^0, \quad \gamma_{\theta z} = \gamma_{\theta z}^0 \tag{2b}$$

where the membrane strains, denoted by ε_r^0, ε_θ^0, $\gamma_{r\theta}^0$, γ_{rz}^0 and $\gamma_{\theta z}^0$, and curvature changes, denoted by κ_r, κ_θ and $\kappa_{r\theta}$, of the reference surface are given as:

$$\begin{aligned} &\varepsilon_r^0 = \frac{\partial u_0}{\partial r}, \kappa_r = \frac{\partial \psi_r}{\partial r}, \quad \varepsilon_\theta^0 = \frac{u_0}{r} + \frac{1}{r}\frac{\partial v_0}{\partial \theta}, \\ &\kappa_\theta = \frac{1}{r}\frac{\partial \psi_\theta}{\partial \theta} + \frac{\psi_r}{r}, \quad \kappa_{r\theta} = \frac{\partial \psi_\theta}{\partial r} + \frac{1}{r}\frac{\partial \psi_r}{\partial \theta} - \frac{\psi_\theta}{r} \end{aligned} \tag{3a}$$

$$\begin{aligned} &\gamma_{rz}^0 = \frac{\partial w}{\partial r} + \psi_r, \gamma_{\theta z}^0 = \frac{1}{r}\frac{\partial w}{\partial \theta} + \psi_\theta, \\ &\gamma_{r\theta}^0 = \frac{\partial v_0}{\partial r} + \frac{1}{r}\frac{\partial u_0}{\partial \theta} - \frac{v_0}{r} \end{aligned} \tag{3b}$$

According to the Hooke's law, the corresponding stress-strain relations of the functionally graded circular, annular and sector plates can be written as:

$$\begin{Bmatrix} \sigma_r \\ \sigma_\theta \\ \tau_{r\theta} \\ \tau_{rz} \\ \tau_{\theta z} \end{Bmatrix} = \begin{bmatrix} \overline{Q}_{11}^k & \overline{Q}_{12}^k & \overline{Q}_{16}^k & 0 & 0 \\ \overline{Q}_{12}^k & \overline{Q}_{22}^k & \overline{Q}_{26}^k & 0 & 0 \\ \overline{Q}_{16}^k & \overline{Q}_{26}^k & \overline{Q}_{66}^k & 0 & 0 \\ 0 & 0 & 0 & \overline{Q}_{44}^k & \overline{Q}_{45}^k \\ 0 & 0 & 0 & \overline{Q}_{45}^k & \overline{Q}_{55}^k \end{bmatrix} \begin{Bmatrix} \varepsilon_r \\ \varepsilon_\theta \\ \gamma_{r\theta} \\ \gamma_{rz} \\ \gamma_{\theta z} \end{Bmatrix} \tag{4}$$

in which σ_r and σ_θ are the normal stresses in the r, θ direction, $\tau_{r\theta}$, τ_{rz} and $\tau_{\theta z}$ are shear stresses in the r, θ and z in the orthogonal cylindrical coordinate system. $\overline{Q}_{ij}^k(i,j$ =1, 2, 4-6) are the lamina stiffness coefficients [56], which are found from following equations:

$$\begin{aligned} \overline{Q}_{11}^k = {} & Q_{11}^k \cos^4 \alpha^k + 2(Q_{12}^k + 2Q_{66}^k) \sin^2 \alpha^k \cos^2 \theta^k \\ & + Q_{22}^k \sin^4 \alpha^k \end{aligned} \tag{5a}$$

$$\begin{aligned} \overline{Q}_{12}^k = {} & (Q_{11}^k + Q_{22}^k - 4Q_{66}^k) \sin^2 \alpha^k \cos^2 \theta^k \\ & + Q_{12}^k(\sin^4 \alpha^k + \cos^4 \alpha^k) \end{aligned} \tag{5b}$$

$$\begin{aligned} \overline{Q}_{12}^k = {} & (Q_{11}^k + Q_{22}^k - 4Q_{66}^k) \sin^2 \alpha^k \cos^2 \alpha^k \\ & + Q_{12}^k(\sin^4 \alpha^k + \cos^4 \alpha^k) \end{aligned} \tag{5c}$$

$$\begin{aligned} \overline{Q}_{16}^k = {} & (Q_{11}^k - Q_{12}^k - 2Q_{66}^k) \cos^3 \alpha^k \sin \alpha^k \\ & + (Q_{12}^k - Q_{22}^k + 2Q_{66}^k) \sin^3 \alpha^k \cos \alpha^k \end{aligned} \tag{5d}$$

$$\overline{Q}_{26}^k = (Q_{11}^k - Q_{12}^k - 2Q_{66}^k)\sin^3\alpha^k\cos\alpha^k + (Q_{12}^k - Q_{22}^k + 2Q_{66}^k)\cos^3\alpha^k\sin\alpha^k \tag{5e}$$

$$\overline{Q}_{66}^k = (Q_{11}^k + Q_{22}^k - 2Q_{12}^k - 2Q_{66}^k)\sin^2\alpha^k\cos^2\alpha^k + Q_{66}^k(\sin^4\alpha^k + \cos^4\alpha^k) \tag{5f}$$

$$\overline{Q}_{44}^k = Q_{44}^k\cos^2\alpha^k + Q_{55}^k\sin^2\alpha^k \tag{5g}$$

$$\overline{Q}_{55}^k = Q_{55}^k\cos^2\alpha^k + Q_{44}^k\sin^2\alpha^k \tag{5h}$$

$$\overline{Q}_{45}^k = (Q_{55}^k - Q_{44}^k)\cos\alpha^k\sin\alpha^k \tag{5i}$$

Where α^k is the fiber orientation angle between the principal direction of the kth orthotropic lamina layer and the r-directions. The Q_{ij} are the plane-stress reduced elastic constants in the material axes of the kth orthotropic lamina:

$$Q_{11}^k = \frac{E_1^k}{1-\mu_{12}^k\mu_{21}^k}, \quad Q_{22}^k = \frac{E_2^k}{1-\mu_{12}^k\mu_{21}^k}, \quad Q_{12}^k = Q_{21}^k = \mu_{21}^k Q_{11}^k \tag{6a}$$

$$Q_{33}^k = G_{12}^k, \quad Q_{44}^k = G_{23}^k, \quad Q_{55}^k = G_{13}^k, \quad \mu_{21}^k = \mu_{12}^k\frac{E_2^k}{E_1^k} \tag{6b}$$

in which E_1, E_2, μ_{12}, μ_{12}, G_{12}, G_{23} and G_{13} are the material properties of the kth orthotropic lamina. It should be noted that by letting $E_1 = E_2$, $G_{12} = G_{13} = G_{23} = E_1(2+2\mu_{12})$, the present analysis can be readily used to analyze isotropic annular sector plates with general boundary conditions ,internal radial line and circumferential supports.

By carrying the integration of the stresses over the cross-section, the force and moment resultants can be obtained:

$$\begin{Bmatrix} N_r \\ N_\theta \\ N_{r\theta} \end{Bmatrix} = b\int_{-h/2}^{h/2}\begin{bmatrix}\sigma_r \\ \sigma_\theta \\ \tau_{r\theta}\end{bmatrix}dz, \quad \begin{Bmatrix} M_r \\ M_\theta \\ M_{r\theta} \end{Bmatrix} = b\int_{-h/2}^{h/2}\begin{bmatrix}\sigma_r \\ \sigma_\theta \\ \tau_{r\theta}\end{bmatrix}zdz \tag{7}$$

$$\begin{Bmatrix} Q_r \\ Q_\theta \end{Bmatrix} = \kappa b\int_{-h/2}^{h/2}\begin{bmatrix}\tau_{rz} \\ \tau_{\theta z}\end{bmatrix}dz \tag{8}$$

where N_r, N_θ and $N_{r\theta}$ are the in-place force resultants, M_r, M_θ and $M_{r\theta}$ are moment resultants, Q_r, Q_θ are transverse shear force resultants. κ is the shear correction coefficient and is taken as κ=5/ 6. Performing the integration operation in Eqs. (7) and (8), the force and moment resultants can be written as:

$$\begin{Bmatrix} N_r \\ N_\theta \\ N_{r\theta} \end{Bmatrix} = \begin{bmatrix} A_{11} & A_{12} & A_{16} \\ A_{12} & A_{22} & A_{26} \\ A_{16} & A_{26} & A_{66} \end{bmatrix}\begin{Bmatrix} \varepsilon_r^0 \\ \varepsilon_\theta^0 \\ \gamma_{r\theta}^0 \end{Bmatrix} + \begin{bmatrix} B_{11} & B_{12} & B_{16} \\ B_{12} & B_{22} & B_{26} \\ B_{16} & B_{26} & B_{66} \end{bmatrix}\begin{Bmatrix} \kappa_r \\ \kappa_\theta \\ \kappa_{r\theta} \end{Bmatrix} \tag{9}$$

$$\begin{Bmatrix} M_r \\ M_\theta \\ M_{r\theta} \end{Bmatrix} = \begin{bmatrix} B_{11} & B_{12} & B_{16} \\ B_{12} & B_{22} & B_{26} \\ B_{16} & B_{26} & B_{66} \end{bmatrix}\begin{Bmatrix} \varepsilon_r^0 \\ \varepsilon_\theta^0 \\ \gamma_{r\theta}^0 \end{Bmatrix} + \begin{bmatrix} D_{11} & D_{12} & D_{16} \\ D_{12} & D_{22} & D_{26} \\ D_{16} & D_{26} & D_{66} \end{bmatrix}\begin{Bmatrix} \kappa_r \\ \kappa_\theta \\ \kappa_{r\theta} \end{Bmatrix} \tag{10}$$

$$\begin{Bmatrix} Q_r \\ Q_\theta \end{Bmatrix} = \kappa\begin{bmatrix} A_{55} & A_{45} \\ A_{45} & A_{44} \end{bmatrix}\begin{bmatrix} \gamma_{rz}^0 \\ \gamma_{\theta z}^0 \end{bmatrix} \tag{11}$$

where A_{ij}, B_{ij} and D_{ij} are the extensional, extensional-bending coupling, bending stiffness, and they are respectively expressed as

$$A_{ij} = \sum_{k=1}^{N}\overline{Q}_{ij}^k(Z_{k+1} - Z_k), \tag{12}$$

$$B_{ij} = \frac{1}{2}\sum_{k=1}^{N}\overline{Q}_{ij}^k(Z_{k+1}^2 - Z_k^2), \quad D_{ij} = \frac{1}{3}\sum_{k=1}^{N}\overline{Q}_{ij}^k(Z_{k+1}^3 - Z_k^3),$$

in which N denotes the amount of the laminas. It should be noted that for the sector plates which are symmetrically with respect to their middle surface, $B_{ij} = 0$.

2.3 Energy expressions

The strain energy (Us) of the functionally graded circular, annular and sector plates during vibration can be define as

$$U_s = \frac{1}{2}\int\int\int_V \begin{Bmatrix} N_r\varepsilon_r^0 + N_\theta\varepsilon_\theta^0 + N_{r\theta}\gamma_{r\theta}^0 + M_r\kappa_r \\ +M_\theta\kappa_\theta + M_{r\theta}\kappa_{r\theta} + Q_r\gamma_{rz}^0 + Q_\theta\gamma_{\theta z}^0 \end{Bmatrix}(s+a)dsd\theta dz \tag{13}$$

Substituting Eqs. (4), (9), (10) and (11) into Eq. (13), the strain energy expression of the structure can be written in

terms of middle plane displacements and rotations.

$$U_s = \frac{1}{2}\int_o^R\int_0^\phi \begin{Bmatrix} A_{11}\left(\frac{\partial u_0}{\partial r}\right)^2 + A_{22}\left(\frac{u_0}{r}+\frac{1}{r}\frac{\partial v_0}{\partial \theta}\right)^2 \\ +A_{66}\left(\frac{\partial v_0}{\partial r}+\frac{1}{r}\frac{\partial u_0}{\partial \theta}-\frac{v_0}{r}\right)^2 \\ +2A_{12}\left(\frac{\partial u_0}{\partial r}\right)\left(\frac{u_0}{r}+\frac{1}{r}\frac{\partial v_0}{\partial \theta}\right) \\ +2A_{26}\left(\frac{u_0}{r}+\frac{1}{r}\frac{\partial v_0}{\partial \theta}\right) \\ \cdot\left(\frac{\partial v_0}{\partial r}+\frac{1}{r}\frac{\partial u_0}{\partial \theta}-\frac{v_0}{r}\right) \\ +2A_{16}\left(\frac{\partial u_0}{\partial r}\right)\left(\frac{\partial v_0}{\partial r}+\frac{1}{r}\frac{\partial u_0}{\partial \theta}-\frac{v_0}{r}\right) \\ +\kappa A_{55}\left(\frac{\partial w}{\partial r}+\psi_r\right)^2 \\ +\kappa A_{44}\left(\frac{1}{r}\frac{\partial w}{\partial \theta}+\psi_\theta\right)^2 \\ +2\kappa A_{45}\left(\frac{\partial w}{\partial r}+\psi_r\right)\left(\frac{1}{r}\frac{\partial w}{\partial \theta}+\psi_\theta\right) \end{Bmatrix}(s+a)dsd\theta \tag{14}$$

$$U_{bs} = \int_o^R\int_0^\phi \begin{Bmatrix} B_{11}\left(\frac{\partial u_0}{\partial r}\right)\left(\frac{\partial \psi_r}{\partial r}\right) \\ +B_{12}\left(\frac{\partial u_0}{\partial r}\right)\left(\frac{1}{r}\frac{\partial \psi_\theta}{\partial \theta}+\frac{\psi_r}{r}\right) \\ +B_{12}\left(\frac{u_0}{r}+\frac{1}{r}\frac{\partial v_0}{\partial \theta}\right)\left(\frac{\partial \psi_r}{\partial r}\right) \\ +B_{12}\left(\frac{\partial u_0}{\partial r}\right)\left(\frac{\partial \psi_\theta}{\partial r}+\frac{1}{r}\frac{\partial \psi_r}{\partial \theta}-\frac{\psi_\theta}{r}\right) \\ +B_{22}\left(\frac{u_0}{r}+\frac{1}{r}\frac{\partial v_0}{\partial \theta}\right)\left(\frac{1}{r}\frac{\partial \psi_\theta}{\partial \theta}+\frac{\psi_r}{r}\right) \\ +B_{16}\left(\frac{\partial v_0}{\partial r}+\frac{1}{r}\frac{\partial u_0}{\partial \theta}-\frac{v_0}{r}\right)\left(\frac{\partial \psi_r}{\partial r}\right) \\ +B_{26}\left(\frac{u_0}{r}+\frac{1}{r}\frac{\partial v_0}{\partial \theta}\right) \\ \cdot\left(\frac{\partial \psi_\theta}{\partial r}+\frac{1}{r}\frac{\partial \psi_r}{\partial \theta}-\frac{\psi_\theta}{r}\right) \\ +B_{26}\left(\frac{\partial v_0}{\partial r}+\frac{1}{r}\frac{\partial u_0}{\partial \theta}-\frac{v_0}{r}\right) \\ \cdot\left(\frac{1}{r}\frac{\partial \psi_\theta}{\partial \theta}+\frac{\psi_r}{r}\right) \\ +B_{26}\left(\frac{\partial v_0}{\partial r}+\frac{1}{r}\frac{\partial u_0}{\partial \theta}-\frac{v_0}{r}\right) \\ \cdot\left(\frac{\partial \psi_\theta}{\partial r}+\frac{1}{r}\frac{\partial \psi_r}{\partial \theta}-\frac{\psi_\theta}{r}\right) \end{Bmatrix}(s+a)dsd\theta \tag{15}$$

$$U_b = \frac{1}{2}\int_o^R\int_0^\phi \begin{Bmatrix} D_{11}\left(\frac{\partial \psi_r}{\partial r}\right)^2 + D_{22}\left(\frac{1}{r}\frac{\partial \psi_\theta}{\partial \theta}+\frac{\psi_r}{r}\right)^2 \\ +D_{66}\left(\frac{\partial \psi_\theta}{\partial r}+\frac{1}{r}\frac{\partial \psi_r}{\partial \theta}-\frac{\psi_\theta}{r}\right)^2 \\ +2D_{12}\left(\frac{\partial \psi_r}{\partial r}\right)\left(\frac{1}{r}\frac{\partial \psi_\theta}{\partial \theta}+\frac{\psi_r}{r}\right) \\ +2D_{16}\left(\frac{\partial \psi_r}{\partial r}\right)\left(\frac{\partial \psi_\theta}{\partial r}+\frac{1}{r}\frac{\partial \psi_r}{\partial \theta}-\frac{\psi_\theta}{r}\right) \\ +2D_{26}\left(\frac{1}{r}\frac{\partial \psi_\theta}{\partial \theta}+\frac{\psi_r}{r}\right) \\ \cdot\left(\frac{\partial \psi_\theta}{\partial r}+\frac{1}{r}\frac{\partial \psi_r}{\partial \theta}-\frac{\psi_\theta}{r}\right) \end{Bmatrix}(s+a)dsd\theta \tag{16}$$

The corresponding kinetic energy (T) function of the laminated annular sector plates can be given as:

$$T = \frac{1}{2}\int_0^R\int_0^\phi\int_{-h/2}^{h/2}\rho\left[\left(\frac{\partial u}{\partial t}\right)^2+\left(\frac{\partial v}{\partial t}\right)^2 + \left(\frac{\partial w}{\partial t}\right)^2\right](s+a)dsd\theta dz \tag{17}$$

Substituting u, v and w from Eq (1) into Eq. (17) and performing the integration with respect to z results in

$$T = \frac{1}{2}\int_0^R\int_0^\phi \begin{Bmatrix} I_0\left[\left(\frac{\partial u_0}{\partial t}\right)^2+\left(\frac{\partial v_0}{\partial t}\right)^2+\left(\frac{\partial w}{\partial t}\right)^2\right] \\ +2I_1\left[\left(\frac{\partial u_0}{\partial t}\right)\left(\frac{\partial \psi_r}{\partial t}\right) \\ +\left(\frac{\partial v_0}{\partial t}\right)\left(\frac{\partial \psi_\theta}{\partial t}\right)\right] \\ +I_2\left[\left(\frac{\partial \psi_r}{\partial t}\right)^2+\left(\frac{\partial \psi_\theta}{\partial t}\right)^2\right] \end{Bmatrix}(s+a)dsd\theta \tag{18}$$

where

$$\begin{pmatrix} I_0 & I_1 & I_2 \end{pmatrix} = \int_{-h/2}^{h/2}\rho\begin{pmatrix} 1 & z & z^2 \end{pmatrix}dz \tag{19}$$

As mentioned in 2.1, to simulate the typical boundary condition, each edge of the plate is restrained by five groups of artificial boundary springs (k_u, k_v, k_w; K_R, K_θ). And the implement of different boundary force on the midplane of the plate is realized by assigning the spring stiffness with various values, which can be from zero to infinity.

Therefore, the deformation strain energy (*Usp*) stored in the boundary springs during vibration can be defined as:

$$U_{sp} = \frac{1}{2}\int_0^\phi \begin{Bmatrix} a\left[k^u_{r\_0}u_0^2 + k^v_{r\_0}v_0^2 \right. \\ \left. +k^w_{r\_0}w^2 + K^R_{r\_0}\psi_r^2 + K^\theta_{r\_0}\psi_\theta^2\right]_{s=0} \\ b\left[k^u_{r\_1}u_0^2 + k^v_{r\_1}v_0^2 \right. \\ \left. +k^w_{r\_1}w^2 + K^R_{r\_1}\psi_r^2 + K^\theta_{r\_1}\psi_\theta^2\right]_{s=R} \end{Bmatrix}d\theta + \frac{1}{2}\int_0^R \begin{Bmatrix} \left[k^u_{\deg\_0}u_0^2 + k^v_{\deg\_0}v_0^2 + k^w_{\deg\_0}w^2 \right. \\ \left. +K^R_{\deg\_0}\psi_r^2 + K^\theta_{\deg\_0}\psi_\theta^2\right]_{\theta=0} \\ \left[k^u_{\deg\_1}u_0^2 + k^v_{\deg\_1}v_0^2 + k^w_{\deg\_1}w^2 \right. \\ \left. +K^R_{\deg\_1}\psi_r^2 + K^\theta_{\deg\_1}\psi_\theta^2\right]_{\theta=\phi} \end{Bmatrix}ds \tag{20}$$

2.4 Governing equations and boundary conditions

The governing equations and boundary conditions of a functionally graded annular sector plates can be obtained by applying the Hamilton's principle. The Lagrangian functional (L) of the plates during vibration can be expressed in terms of the energy expressions as:

$$L = T - U_s - U_b - U_{bs} - U_{sp} \tag{21}$$

Substituting Eqs. (14)–(20) into Eq. (21) and applying the Hamilton's principle:

$$\delta \int_0^t (T - U_s - U_{sp} - U_{cp})\, dt = 0 \tag{22}$$

yields:

$$\int_0^t \int_0^{\phi} \left\{ \begin{array}{l} a\left[k^u_{r\_0} u_0 \delta u_0 + k^v_{r\_0} v_0 \delta v_0 \right. \\ \left. + k^w_{r\_0} w \delta w + K^R_{r\_0} \psi_r \delta \psi_r + K^{\theta}_{r\_0} \psi_\theta \delta \psi_\theta \right]_{s=0} \\ b\left[k^u_{r\_1} u_0 \delta u_0 + k^v_{r\_1} v_0 \delta v_0 \right. \\ \left. + k^w_{r\_1} w \delta w + K^R_{r\_1} \psi_r \delta \psi_r + K^{\theta}_{r\_1} \psi_\theta \delta \psi_\theta \right]_{s=R} \end{array} \right\} d\theta dt$$

$$+ \int_0^t \int_0^R \left\{ \begin{array}{l} \left[k^u_{\deg\_0} u_0 \delta u_0 + k^v_{\deg\_0} v_0 \delta v_0 \right. \\ + k^w_{\deg\_0} w \delta w + K^R_{\deg\_0} \psi_r \delta \psi_r \\ \left. + K^{\theta}_{\deg\_0} \psi_\theta \delta \psi_\theta \right]_{\theta=0} \\ \left[k^u_{\deg\_1} u_0 \delta u_0 + k^v_{\deg\_1} v_0 \delta v_0 \right. \\ + k^w_{\deg\_1} w \delta w + K^R_{\deg\_1} \psi_r \delta \psi_r \\ \left. + K^{\theta}_{\deg\_1} \psi_\theta \delta \psi_\theta \right]_{\theta=\phi} \end{array} \right\} ds dt$$

$$+ \int_0^t \int\int_s \left\{ \begin{array}{l} N_r \frac{\partial \delta u_0}{\partial r} + N_\theta \left(\frac{\delta u_0}{r} + \frac{1}{r} \frac{\partial \delta v_0}{\partial \theta} \right) \\ + N_{r\theta} \left(\frac{\partial \delta v_0}{\partial r} + \frac{1}{r} \frac{\partial \delta u_0}{\partial \theta} - \frac{\delta v_0}{r} \right) \\ + M_r \frac{\partial \delta \psi_r}{\partial r} \\ + M_\theta \left(\frac{1}{r} \frac{\partial \delta \psi_\theta}{\partial \theta} + \frac{\delta \psi_r}{r} \right) \\ + Q_\theta \left(\frac{1}{r} \frac{\partial \delta w}{\partial \theta} + \delta \psi_\theta \right) \\ M_{r\theta} \left(\frac{\partial \delta \psi_\theta}{\partial r} + \frac{1}{r} \frac{\partial \delta \psi_r}{\partial \theta} - \frac{\delta \psi_\theta}{r} \right) \\ + Q_r \left(\frac{\partial \delta w}{\partial r} + \delta \psi_r \right) \end{array} \right\} (s+a) ds d\theta dt$$

$$- \int_0^t \int\int_s \left\{ \begin{array}{l} I_0 \left[\frac{\partial u_0}{\partial t} \frac{\partial \delta u_0}{\partial t} + \frac{\partial v_0}{\partial t} \frac{\partial \delta v_0}{\partial t} \right. \\ \left. + \frac{\partial w}{\partial t} \frac{\partial \delta w}{\partial t} \right] \\ + I_1 \left[\frac{\partial u_0}{\partial t} \frac{\partial \delta \psi_r}{\partial t} + \frac{\partial \delta u_0}{\partial t} \frac{\partial \psi_r}{\partial t} \right. \\ \left. + \frac{\partial \delta v_0}{\partial t} \frac{\partial \psi_\theta}{\partial t} + \frac{\partial v_0}{\partial t} \frac{\partial \delta \psi_\theta}{\partial t} \right] \\ + I_2 \left[\frac{\partial \psi_r}{\partial t} \frac{\partial \delta \psi_r}{\partial t} + \frac{\partial \psi_\theta}{\partial t} \frac{\partial \delta \psi_\theta}{\partial t} \right] \end{array} \right\} (s+a) ds d\theta dt \tag{23}$$

Integrating by parts to relieve the virtual displacements δu_0, δv_0, δw, $\delta_{\psi r}$ and $\delta_{\psi\theta}$ we have:

$$+ \int_0^t \int_0^{\phi} \left\{ \begin{array}{l} \left[a\left(N_r + k^u_{r\_0} u_0\right)|_{r=0} \right. \\ \left. - b\left(N_r - k^u_{r\_1} u_0\right)|_{r=R}\right] \delta u_0 \\ + \left[a\left(N_{r\theta} + k^v_{r\_0} v_0\right)|_{r=0} \right. \\ \left. - b\left(N_{r\theta} - k^v_{r\_1} v\right)|_{r=R}\right] \delta v_0 \\ + \left[a\left(Q_r + k^w_{r\_0} w\right)|_{r=0} \right. \\ \left. - b\left(Q_r - k^w_{r\_1} w\right)|_{r=R}\right] \delta w \\ + \left[a\left(M_r + K^R_{r\_0} \psi_r\right)|_{r=0} \right. \\ \left. - b\left(M_r - K^R_{r\_1} \psi_r\right)|_{r=R}\right] \delta \psi_r \\ + \left[a\left(M_{r\theta} + K^{\theta}_{r\_0} \psi_\theta\right)|_{r=0} \right. \\ \left. - b\left(M_{r\theta} - K^{\theta}_{r\_1} \psi_\theta\right)|_{r=R}\right] \delta \psi_\theta \end{array} \right\} d\theta dt$$

$$0 = \int_0^t \int\int_s \left\{ \begin{array}{l} \frac{\partial N_r}{\partial r} + \frac{\partial N_{r\theta}}{r \partial \theta} - \frac{N_\theta}{r} \\ - I_0 \left(\frac{\partial u_0}{\partial t} \right)^2 - I_1 \left(\frac{\partial \psi_r}{\partial t} \right)^2 \end{array} \right\} \delta u_0 (s+a) ds d\theta dt$$

$$+ \int_0^t \int\int_s \left\{ \begin{array}{l} \frac{\partial N_\theta}{r \partial \theta} + \frac{\partial N_{r\theta}}{\partial r} + \frac{N_{r\theta}}{r} \\ - I_0 \left(\frac{\partial v_0}{\partial t} \right)^2 - I_1 \left(\frac{\partial \psi_\theta}{\partial t} \right)^2 \end{array} \right\} \delta v_0 (s+a) ds d\theta dt$$

$$+ \int_0^t \int\int_s \left\{ \frac{\partial Q_r}{\partial r} + \frac{\partial Q_\theta}{r \partial \theta} - I_0 \left(\frac{\partial w}{\partial t} \right)^2 \right\} \delta w (s+a) ds d\theta dt$$

$$+ \int_0^t \int\int_s \left\{ \begin{array}{l} \frac{\partial M_r}{\partial r} + \frac{\partial M_{r\theta}}{r \partial \theta} - \frac{M_\theta}{r} - Q_r \\ - I1 \left(\frac{\partial u_0}{\partial t} \right)^2 - I2 \left(\frac{\partial \psi_r}{\partial t} \right)^2 \end{array} \right\} \delta \psi_r (s+a) ds d\theta dt$$

$$+ \int_0^t \int\int_s \left\{ \begin{array}{l} \frac{\partial M_\theta}{r \partial \theta} + \frac{\partial M_{r\theta}}{\partial r} + \frac{M_{r\theta}}{r} - Q_\theta \\ - I_1 \left(\frac{\partial v_0}{\partial t} \right)^2 - I_2 \left(\frac{\partial \psi_\theta}{\partial t} \right)^2 \end{array} \right\} \delta \psi_\theta (s+a) ds d\theta dt$$

$$+ \int_0^t \int_0^R \left\{ \begin{array}{l} \left[\left(N_{r\theta} + k^u_{\deg\_0} u_0\right)|_{\theta=0} \right. \\ \left. - \left(N_{r\theta} - k^u_{\deg\_1} u_0\right)|_{\theta=\phi}\right] \delta u_0 \\ + \left[\left(N_\theta + k^v_{\deg\_0} v_0\right)|_{\theta=0} \right. \\ \left. - \left(N_\theta - k^v_{\deg\_1} v_0\right)|_{\theta=\phi}\right] \delta v_0 \\ + \left[\left(Q_\theta + k^w_{\deg\_0} w\right)|_{\theta=0} \right. \\ \left. - \left(Q_\theta - k^w_{\deg\_1} w\right)|_{\theta=\phi}\right] \delta w \\ + \left[\left(M_{r\theta} + K^R_{\deg\_0} \psi_r\right)|_{\theta=0} \right. \\ \left. - \left(M_{r\theta} - K^R_{\deg\_1} \psi_r\right)|_{\theta=\phi}\right] \delta \psi_r \\ + \left[\left(M_\theta + K^{\theta}_{\deg\_0} \psi_\theta\right)|_{\theta=0} \right. \\ \left. - \left(M_\theta - K^{\theta}_{\deg\_1} \psi_\theta\right)|_{\theta=\phi}\right] \delta \psi_\theta \end{array} \right\} ds dt \tag{24}$$

Since the virtual displacements δ_{u0}, δ_{v0}, δ_w, $\delta_{\psi r}$ and $\delta_{\psi\theta}$ are arbitrary, the Eq. (24) can be satisfied only if the coefficients of the virtual displacements are zero. Thus, the governing equations of the functionally graded annular

sector plates are obtained as

$$\frac{\partial N_r}{\partial r}+\frac{\partial N_{r\theta}}{r\partial\theta}-\frac{N_\theta}{r}=I_0\left(\frac{\partial u_0}{\partial t}\right)^2+I_1\left(\frac{\partial \psi_r}{\partial t}\right)^2 \tag{25a}$$

$$\frac{\partial N_\theta}{r\partial\theta}+\frac{\partial N_{r\theta}}{\partial r}+\frac{N_{r\theta}}{r}=I_0\left(\frac{\partial v_0}{\partial t}\right)^2+I_1\left(\frac{\partial \psi_\theta}{\partial t}\right)^2 \tag{25b}$$

$$\frac{\partial Q_r}{\partial r}+\frac{\partial Q_\theta}{r\partial\theta}=I_0\left(\frac{\partial w}{\partial t}\right)^2 \tag{25c}$$

$$\begin{aligned}&\frac{\partial M_r}{\partial r}+\frac{\partial M_{r\theta}}{r\partial\theta}-\frac{M_\theta}{r}-Q_r\\&=I_1\left(\frac{\partial u_0}{\partial t}\right)^2+I_2\left(\frac{\partial \psi_r}{\partial t}\right)^2\end{aligned} \tag{25d}$$

$$\begin{aligned}&\frac{\partial M_\theta}{r\partial\theta}+\frac{\partial M_{r\theta}}{\partial r}+\frac{M_{r\theta}}{r}-Q_\theta\\&=I_1\left(\frac{\partial v_0}{\partial t}\right)^2+I_2\left(\frac{\partial \psi_\theta}{\partial t}\right)^2\end{aligned} \tag{25e}$$

Similarly, the general boundary conditions can be written as:

$$s=0:\begin{cases}N_r+k^u_{r\_0}u_0=0\\N_{r\theta}+k^v_{r\_0}v_0=0\\Q_r+k^w_{r\_0}w=0\\M_r+K^R_{r\_0}\psi_r=0\\M_{r\theta}+K^\theta_{r\_0}\psi_\theta=0\end{cases}, \tag{26a}$$

$$s=R:\begin{cases}N_r-k^u_{r\_1}u_0=0\\N_{r\theta}-k^v_{r\_1}v=0\\Q_r-k^w_{r\_1}w=0\\M_r-K^R_{r\_1}\psi_r=0\\M_{r\theta}-K^\theta_{r\_1}\psi_\theta=0\end{cases}$$

$$\theta=0:\begin{cases}N_{r\theta}+k^u_{\mathrm{deg}\_0}u_0=0\\N_\theta+k^v_{\mathrm{deg}\_0}v_0=0\\Q_\theta+k^w_{\mathrm{deg}\_0}w=0\\M_{r\theta}+K^R_{\mathrm{deg}\_0}\psi_r=0\\M_\theta+K^\theta_{\mathrm{deg}\_0}\psi_\theta=0\end{cases}, \tag{26b}$$

$$\theta=\phi:\begin{cases}N_{r\theta}-k^u_{\mathrm{deg}\_1}u_0=0\\N_\theta-k^v_{\mathrm{deg}\_1}v_0=0\\Q_\theta-k^w_{\mathrm{deg}\_1}w=0\\M_{r\theta}-K^R_{\mathrm{deg}\_1}\psi_r=0\\M_\theta-K^\theta_{\mathrm{deg}\_1}\psi_\theta=0\end{cases}$$

2.5 Admissible displacement functions

Because of its simplicity and high accuracy, Rayleigh-Ritz method is widely used in the vibration analysis of structural elements as a very powerful tool. In the Rayleigh-Ritz method, the solutions can be obtained by minimizing the energy functional with respect to the coefficients of the admissible functions. So how to choose the proper admissible functions is the core of study, for it plays the biggest factor in determining the accuracy and stability of the Rayleigh-Ritz method.

The main purpose of the present study is to provide an efficient solution capable of dealing with general boundary conditions, internal radial line and circumferential supports. To satisfy the request, the displacement and rotation components of the sector plate, regardless of boundary conditions, are invariantly expressed as a new form of trigonometric series expansions in which several supplementary terms are introduced to ensure and accelerate the convergence of the series expansion:

$$\begin{aligned}u_0(s,\theta,t)&=U_0(s,\theta)e^{j\omega t}\\&=\left(\sum_{m=0}^{\infty}\sum_{n=0}^{\infty}A_{mn}\cos\lambda_{Rm}s\cos\lambda_{\phi n}\theta\right.\\&+\sum_{l=1}^{2}\zeta_b^l(\theta)\sum_{m=0}^{\infty}a_m^l\cos\lambda_{Rm}s\\&\left.+\sum_{l=1}^{2}\zeta_a^l(s)\sum_{n=0}^{\infty}b_n^l\cos\lambda_{\phi n}\theta\right)e^{j\omega t},\end{aligned} \tag{27a}$$

$$\begin{aligned}v_0(s,\theta,t)&=V_0(s,\theta)e^{j\omega t}\\&=\left(\sum_{m=0}^{\infty}\sum_{n=0}^{\infty}B_{mn}\cos\lambda_{Rm}s\cos\lambda_{\phi n}\theta\right.\\&+\sum_{l=1}^{2}\zeta_b^l(\theta)\sum_{m=0}^{\infty}c_m^l\cos\lambda_{Rm}s\\&\left.+\sum_{l=1}^{2}\zeta_a^l(s)\sum_{n=0}^{\infty}d_n^l\cos\lambda_{\phi n}\theta\right)e^{j\omega t},\end{aligned} \tag{27b}$$

$$\begin{aligned}w(s,\theta,t)&=W(s,\theta)e^{j\omega t}\\&=\left(\sum_{m=0}^{\infty}\sum_{n=0}^{\infty}C_{mn}\cos\lambda_{Rm}s\cos\lambda_{\phi n}\theta\right.\\&+\sum_{l=1}^{2}\zeta_b^l(\theta)\sum_{m=0}^{\infty}e_m^l\cos\lambda_{Rm}s\\&\left.+\sum_{l=1}^{2}\zeta_a^l(s)\sum_{n=0}^{\infty}f_n^l\cos\lambda_{\phi n}\theta\right)e^{j\omega t},\end{aligned} \tag{27c}$$

$$\psi_r(s,\theta,t) = \psi_r(s,\theta)e^{j\omega t} \tag{27d}$$
$$= \left(\sum_{m=0}^{\infty}\sum_{n=0}^{\infty} D_{mn}\cos\lambda_{Rm}s\cos\lambda_{\phi n}\theta + \sum_{l=1}^{2}\zeta_b^l(\theta)\sum_{m=0}^{\infty} g_m^l\cos\lambda_{Rm}s + \sum_{l=1}^{2}\zeta_a^l(s)\sum_{n=0}^{\infty} h_n^l\cos\lambda_{\phi n}\theta\right)e^{j\omega t},$$

$$\psi_\theta(s,\theta,t) = \psi_\theta(s,\theta)e^{j\omega t} \tag{27e}$$
$$= \left(\sum_{m=0}^{\infty}\sum_{n=0}^{\infty} E_{mn}\cos\lambda_{Rm}s\cos\lambda_{\phi n}\theta + \sum_{l=1}^{2}\zeta_b^l(\theta)\sum_{m=0}^{\infty} k_m^l\cos\lambda_{Rm}s + \sum_{l=1}^{2}\zeta_a^l(s)\sum_{n=0}^{\infty} q_n^l\cos\lambda_{\phi n}\theta\right)e^{j\omega t},$$

where $\lambda_{Rm} = m\pi/R$, $\lambda_{\phi n} = n\pi/\phi$, and A_{mn}, B_{mn}, C_{mn}, D_{mn}, E_{mn} are the Fourier coefficients of two-dimensional Fourier series expansions for the displacements functions, respectively. a_m^l, b_n^l, c_m^l, d_n^l, e_m^l, f_n^l, g_m^l, h_n^l, k_m^l, q_n^l are the supplemented coefficients of the auxiliary functions, where l=1, 2. ζ_a^l, ζ_b^l, l=1, 2, represent a set of closed-form sufficiently smooth functions defined over S:([0, R]×[0, ϕ]).

As mentioned above, the potential discontinuities of the original displacements and their derivatives existed in the plate domain can be eliminated by the supplementary terms introduced in the Fourier series, which can accelerate the convergence of the results. According to Eq. (25), there are two derivatives at most in the displacement components, which means that at least two-order derivatives of the admissible functions are required to satisfy the continuities of any point on the plate. To satisfy such requirements, the following simple auxiliary functions are selected:

$$\xi_a^1(s) = \frac{R}{2\pi}\sin\left(\frac{\pi s}{2R}\right) + \frac{R}{2\pi}\sin\left(\frac{3\pi s}{2R}\right) \tag{28a}$$

$$\xi_a^2(s) = -\frac{R}{2\pi}\cos\left(\frac{\pi s}{2R}\right) + \frac{R}{2\pi}\cos\left(\frac{3\pi s}{2R}\right) \tag{28b}$$

It is easy to verify that

$$\xi_a^1(0) = \xi_a^1(R) = \xi_a^{1\prime}(R) = 0,\ \xi_a^{1\prime}(0) = 1 \tag{29a}$$

$$\xi_a^2(0) = \xi_a^2(R) = \xi_a^{2\prime}(0) = 0,\ \xi_a^{2\prime}(R) = 1 \tag{29b}$$

Similar conditions exist for the θ-related polynomials $\zeta_b^1(\theta)$and $\zeta_b^2(\theta)$. Though these conditions are not necessary, they, which can be regarded as the first-order derivatives of the displacement function at the edges, make the one-dimensional Fourier series expansions understandable. Thus the two-dimensional series are formed into residual displacement functions that at least one continuous derivative with respect to s- and θ-directions exists. The series expansion given in Eq. (27) is able to expand and uniformly converge to any function $\Xi(s,\theta) \in C^1$ for S:([0, R]×[0, ϕ]), which can be proven mathematically. Besides, uniformly convergent series can be obtained by differentiations of the series term by term. Arbitrary accuracy of the solution can be achieved theoretically by adopting different truncation methods. In this solution, results with acceptable accuracy are obtained by selecting M and N terms of the series expressions.

2.6 Solution procedure

The coefficients of the admissible functions are to be determined after establishing the admissible displacement functions and energy functions of the plate. Substituting Eqs. (1)-(12) and Eqs. (14)-(20) into Eq. (21) and performing the Rayleigh-Ritz procedure with respect to each unknown coefficient, the motion equation of plate can be yielded and is given in the following matrix form:

$$\left\{\begin{bmatrix} K_{uu} & K_{uv} & 0 & K_{u\psi_r} & K_{u\psi_\theta} \\ K_{vu} & K_{vv} & 0 & K_{v\psi_r} & K_{v\psi_\theta} \\ 0 & 0 & K_{ww} & K_{w\psi_r} & K_{w\psi_r} \\ K_{u\psi_r} & K_{v\psi_r} & K_{w\psi_r} & K_{\psi_r\psi_r} & K_{\psi_r\psi_\theta} \\ K_{u\psi_\theta} & K_{v\psi_\theta} & K_{w\psi_r} & K_{\psi_r\psi_\theta} & K_{\psi_\theta\psi_\theta} \end{bmatrix} - \omega^2\begin{bmatrix} M_{uu} & 0 & 0 & M_{u\psi_r} & 0 \\ 0 & M_{vv} & 0 & 0 & M_{v\psi_\theta} \\ 0 & 0 & M_{ww} & 0 & 0 \\ M_{u\psi_r} & 0 & 0 & M_{\psi_r\psi} & 0 \\ 0 & M_{v\psi_\theta} & 0 & 0 & M_{\psi_\theta\psi_\theta} \end{bmatrix}\right\}\begin{Bmatrix} G_u \\ G_v \\ G_w \\ G_{\psi_r} \\ G_{\psi_\theta} \end{Bmatrix} = 0 \tag{30}$$

where

$$G_u = \begin{Bmatrix} A_{00}, A_{01}, \cdots, A_{m'0}, A_{m'1}, \cdots, A_{m'n'}, \cdots, A_{MN}, \\ a_0^1, \cdots, a_M^1, a_0^2, \cdots, a_M^2, b_0^1, \cdots, b_N^1, b_0^2, \cdots b_N^2 \end{Bmatrix} \tag{31a}$$

$$G_v = \begin{Bmatrix} B_{00}, B_{01}, \cdots, B_{m'0}, B_{m'1}, \cdots, B_{m'n'}, \cdots, B_{MN}, \\ c_0^1, \cdots, c_M^1, c_0^2, \cdots, c_M^2, d_0^1, \cdots, d_N^1, d_0^2, \cdots d_N^2 \end{Bmatrix} \tag{31b}$$

$$G_w = \begin{Bmatrix} C_{00}, C_{01}, \cdots, C_{m'0}, C_{m'1}, \cdots, C_{m'n'}, \cdots, C_{MN}, \\ e_0^1, \cdots, e_M^1, e_0^2, \cdots, e_M^2, ef_0^1, \cdots, f_N^1, f_0^2, \cdots f_N^2 \end{Bmatrix} \tag{31c}$$

$$G_{\psi_r} = \begin{Bmatrix} D_{00}, D_{01}, \cdots, D_{m'0}, D_{m'1}, \cdots, D_{m'n'}, \cdots, D_{MN}, \\ g_0^1, \cdots, g_M^1, g_0^2, \cdots, g_M^2, h_0^1, \cdots, h_N^1, h_0^2, \cdots h_N^2 \end{Bmatrix} \tag{31d}$$

$$G_{\psi_\theta} = \begin{Bmatrix} E_{00}, E_{01}, \cdots, E_{m'0}, E_{m'1}, \cdots, E_{m'n'}, \cdots, E_{MN}, \\ k_0^1, \cdots, k_M^1, k_0^2, \cdots, k_M^2, q_0^1, \cdots, q_N^1, q_0^2, \cdots q_N^2 \end{Bmatrix} \tag{31e}$$

$\mathbf{K}_{ij}$ and $\mathbf{M}_{ij}$ (i, j =u, v, w, Ψ_r and Ψ_θ) are the submatrixes of global stiffness and mass matrices, and the elements of the typical matrices $\mathbf{K}_{uu}$ and $\mathbf{M}_{uu}$ are given in Appendix A.

To obtain the frequencies (or eigenvalues) of composite laminated annular sector plates, only solve the Eq. (30) directly. And further by substituting the corresponding eigenvectors into series representations of displacement and rotation components, the corresponding mode shapes can be yielded.

3 Numerical results and discussion

In this section, a systematic comparison between the current solutions and theoretical results published by other researchers is carried out to validate the excellent accuracy, reliability and feasibility of the present method. Furthermore, the effects of elastic restraint parameters, layout schemes and locations of radial line supports are also reported. New results are obtained for laminated annular sector plates subjected to elastic boundary restraints and arbitrary internal radial line and circumferential arc supports in s and θ directions. The discussion is arranged as: Firstly, the boundary conditions of the sector plate are defined in terms of boundary spring parameters; Secondly, convergence of the modified Fourier solution is tested; Thirdly, the composite laminated annular sector plates with various classical boundary conditions, elastic boundary conditions and their combinations are studied; Then, the effect of layout schemes is reported; Finally, free vibration characteristics of composite laminated annular sector plates with arbitrary internal radial line and circumferential arc supports are analyzed, and the influence of the locations of line supports on the frequency parameters is also studied.

3.1 Determination of the boundary spring stiffness

In this paper, virtual springs applied on the boundaries of the structures are used to simulate the practical boundary forces and displacement, where the general boundary conditions for the structure are achieved. General boundary conditions can be simply obtained by setting desired stiffness of the springs. For example, a clamped boundary conditions (C) can be obtained by setting the stiffness of all the springs to be infinitely large value compared with the rigidities of the structures. In the solution procedure, the "infinitely large" number, which cannot be calculated, is replaced by a finite but large enough number. Therefore, it is necessary to study the influence of the spring stiffness on the modal characteristic of the plate.

In the first example, effects of elastic boundary restraint parameters on the frequency parameters $\Omega = \omega b^2/h(\rho_m/E_2)^{1/2}$ of composite laminated sector annular plate is studied. The geometric and material properties are a/b=0.5, h/b=0.1, $E_1/E_2 = 15$, $E_2 = 1\times10^{10}$Pa, $G_{12} = G_{13} = 0.6E_2$, $G_{23} = 0.5E_2$, $\mu_{12} = 0.25$ and $\rho = 1500$ kg/m^3. For simplicity and convenience in the analysis, five elastic restraint parameters Γ_u, Γ_v, Γ_w, Γ_R and Γ_θ, which are defined as the ratios of the corresponding spring stiffnesses to the flexural stiffness $D = E_2h^3/12(1-\mu_{12}^2)$ are pre-defined here, namely, $\Gamma_u = k_u/D$, $\Gamma_v = k_v/D$, $\Gamma_w = k_w/D$, $\Gamma_R = K_R/D$ and $\Gamma_{x_v} = K_\theta/D$. Also, a frequency parameter $\Delta\Omega$ which is defined as the difference of the non-dimensional frequency parameter $\Omega = \omega b^2/h(\rho_m/E_2)^{1/2}$ to those of the elastic restraint parameters Γ_λ ($\lambda = u, v, w, R$ and θ) equal to 10^{-8}, *i.e.*, $\Delta\Omega = \Omega_{r_1} - \Omega_{r_\lambda} = 10^{-8}$ is used in the calculation. In Figs. 2 and 3, variation of the lowest three frequency parameters $\Delta\Omega$ versus the elastic restraint parameters Γ_λ (λ = u, v, w, R and θ) for unsymmetrically laminated annular sector plates [$0^o/90^o$] and symmetrically laminated annular sector plates [$0^o/90^o/0^o$] are presented, respectively. The considered boundary condition is completely free at boundaries s= 0, s= R, and clamped at boundary θ = 0, while at edge $\theta = \phi$, the plates are elastically supported by only one group of spring component with stiffness varying from $10^{-8}D$ to $10^{10}D$. From Figs. 2-3, it is observed that the frequency parameters $\Delta\Omega$ increase as the stiffness parameters increase in the certain range. It is obvious that the active ranges of stiffness parameters vary with the change of boundary springs. Therefore, the completely clamped boundary conditions of a sector plate can be realized by assigning the boundary spring stiffness to 10^8D.

In the following discussion, the results of vibration characteristics including the frequencies and the modal shapes of the composite laminated sector plate are presented. The boundary conditions considered here includes various classical boundary conditions, general boundary conditions and the combinations of both the two kinds of boundary conditions. The spring stiffness parameter corresponding to three kinds of classical boundary conditions and three kinds of general elastic boundary conditions which are commonly used in the practical situation for

Table 1: Convergence of the first six frequency parameters for a [0°/90°] laminated annular sector plate with CCCC and FFFF boundary conditions (ϕ=2π/3, a/b=0.5, h/b=0.2, E_1/E_2=40)

$M\times N$	CCCC						FFFF					
	1	2	3	4	5	6	1	2	3	4	5	6
8×8	5.175	5.694	6.619	7.810	9.153	10.027	1.318	1.455	2.608	2.662	3.442	4.163
9×9	5.175	5.694	6.619	7.809	9.153	10.027	1.318	1.455	2.607	2.662	3.442	4.162
10×10	5.175	5.694	6.619	7.809	9.151	10.027	1.318	1.455	2.607	2.662	3.441	4.162
11×11	5.175	5.694	6.619	7.809	9.151	10.027	1.318	1.455	2.607	2.661	3.441	4.162
12×12	5.175	5.694	6.619	7.809	9.150	10.027	1.318	1.455	2.607	2.661	3.441	4.162
13×13	5.175	5.694	6.619	7.809	9.150	10.027	1.318	1.455	2.606	2.661	3.441	4.161
14×14	5.175	5.694	6.619	7.809	9.150	10.026	1.318	1.455	2.606	2.661	3.441	4.161
15×15	5.175	5.694	6.619	7.809	9.150	10.026	1.318	1.455	2.606	2.661	3.441	4.161
16×16	5.175	5.694	6.619	7.809	9.150	10.026	1.318	1.455	2.606	2.661	3.441	4.161

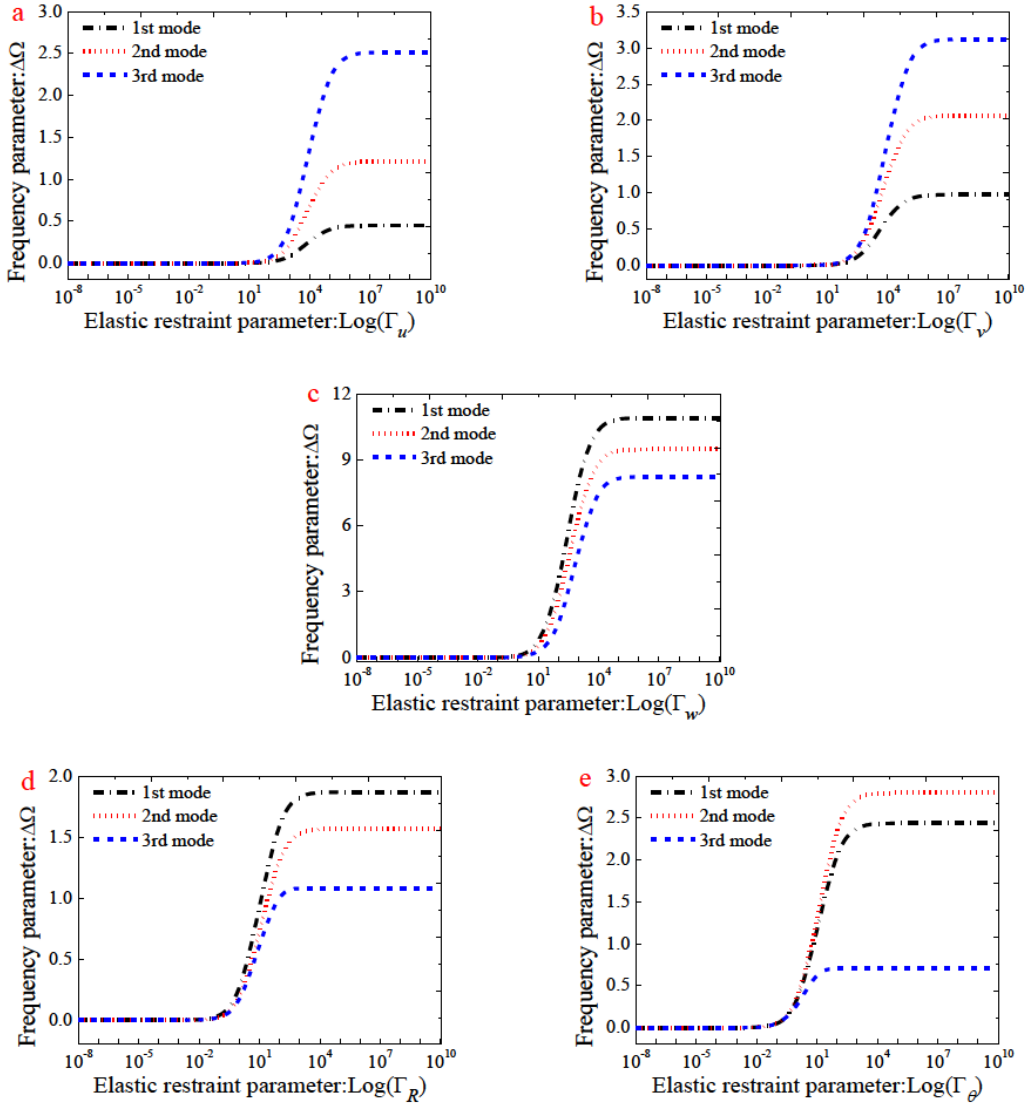

Figure 2: Variation of the frequency parameters $\Delta\Omega$ versus the elastic restraint parameters Γ_λ for a two-layered, [0^o/90°], unsymmetrically laminated annular sector plate: (a) Γ_u; (b) Γ_v; (c) Γ_w; (d) Γ_R; and (e) Γ_θ

Table 2: Comparison of the frequency parameters Ω for a $[0^\circ/90^\circ]_5$ laminated annular sector plate with different classical boundary conditions ($\phi = \pi/3$, a/b=0.1, h/b=0.2, E_1/E_2=40).

B.C	Solutions	Mode					
		1	2	3	4	5	6
CCCC	Presnet	16.808	25.668	25.944	34.775	35.496	35.901
	DQM[18]	16.912	25.827	26.103	34.996	35.719	36.125
	Error(%)	0.619	0.619	0.612	0.634	0.629	0.623
SSSS	Presnet	12.363	15.183	17.779	22.996	25.050	25.517
	DQM[18]	12.363	15.256	17.874	22.997	25.194	25.666
	Error(%)	0.001	0.482	0.533	0.004	0.573	0.584
CSCS	Presnet	12.363	15.742	22.996	25.131	25.815	33.718
	DQM[18]	12.363	15.828	22.997	25.28	25.971	33.719
	Error(%)	0.001	0.549	0.004	0.592	0.603	0.004
CSSS	Presnet	12.363	15.244	22.996	23.393	25.112	25.523
	DQM[18]	12.363	15.321	22.997	23.409	25.26	25.672
	Error(%)	0.001	0.504	0.004	0.067	0.589	0.585

edge s=0 are given as

$$\text{B.C.}\begin{cases} \text{C}: \begin{bmatrix} u_0=0, v_0=0, w=0, \psi_r=0, \psi_\theta=0 \\ k^u_{r\_0}=10^7 D_m, k^v_{r\_0}=10^8 D, k^w_{r\_0}=10^8 D, \\ K^R_{r\_0}=10^8 D, K^\theta_{r\_0}=10^8 D \end{bmatrix} \\ \text{F}: \begin{bmatrix} N_r=0, N_{r\theta}=0, Q_r=0, M_r=0, M_{r\theta}=0 \\ k^u_{r\_0}=0, k^v_{r\_0}=0, k^w_{r\_0}=0, K^R_{r\_0}=0, K^\theta_{r\_0}=0 \end{bmatrix} \\ \text{S}: \begin{bmatrix} N_r=0, v_0=0, w=0, M_r=0, \psi_\theta=0 \\ k^u_{r\_0}=0, k^v_{r\_0}=10^8 D, k^w_{r\_0}=10^8 D, \\ K^R_{r\_0}=0, K^\theta_{r\_0}=110^8 D \end{bmatrix} \\ \text{E}^1: \begin{bmatrix} u_0\neq 0, v_0\neq 0, w=0, \psi_r=0, \psi_\theta=0 \\ k^u_{r\_0}=10^2 D, k^v_{r\_0}=10^2 D, k^w_{r\_0}=10^8 D, \\ K^R_{r\_0}=10^8 D, K^\theta_{r\_0}=10^8 D \end{bmatrix} \\ \text{E}^2: \begin{bmatrix} u_0=0, v_0=0, w\neq 0, \psi_r=0, \psi_\theta=0 \\ k^u_{r\_0}=10^8 D, k^v_{r\_0}=10^8 D, k^w_{r\_0}=10^2 D, \\ K^R_{r\_0}=10^8 D, K^\theta_{r\_0}=10^8 D \end{bmatrix} \\ \text{E}^3: \begin{bmatrix} u_0=0, v_0=0, w=0, \psi_r\neq 0, \psi_\theta\neq 0 \\ k^u_{r\_0}=10^8 D, k^v_{r\_0}=10^8 D, k^w_{r\_0}=10^8 D, \\ K^R_{r\_0}=10^2 D, K^\theta_{r\_0}=10^2 D \end{bmatrix} \end{cases}$$

To test the appropriateness of this definition, namely, express the classical boundary conditions in terms of boundary spring parameters, several numerical examples will be conducted in later sub-sections. For reasons of brevity, a brief letter string is used to express the boundary condition of the laminated annular sector plate, such as FCSC denotes the annular sector plate with F, C, S and C boundary conditions at boundaries $s = 0$, $\theta = 0$, $s = R$ and $\theta = \phi$, respectively. Unless otherwise stated, the natural frequencies of the laminated annular sector plates are expressed in the non-dimensional parameters as $\Omega = \omega b^2/h(\rho_m/E_2)^{1/2}$ and the material properties of the plates are given as: $E_2 = 1 \times 10^{10}$Pa, $E_1/E_2 = 15$, $G_{12} = G_{13} = 0.6E_2$, $G_{23} = 0.5E_2$, $\mu_{12} = 0.25$ and ρ=1500 kg/m^3.

3.2 Convergence study

In this sub-section, the convergence of composite laminated annular sector plates with different boundary conditions is studied. Table 1 shows the convergence studies made for the first six frequency parameters Ω of a moderately thick, two-layered laminated $[0^\circ/90^\circ]$) annular sector plates with different boundary conditions, *i.e.* CCCC and FFFF. The solutions for truncation schemes M=N=8, 9, 10, 11, 12, 13,14,15 and 16 are included in studies. It is obvious that the present method converges excellently and the results are accurate enough even with a small truncated number. The maximum difference between the results of M=N=8 and those of M=N=16 is less than 0.078% for the worst situation. Therefore, the truncated numbers for the Fourier series are set as M=N=12 for the following examples, which are presented to further demonstrate the accuracy and reliability of the present method. For each example, the results of convergence study are given in detail while only the converged results are given.

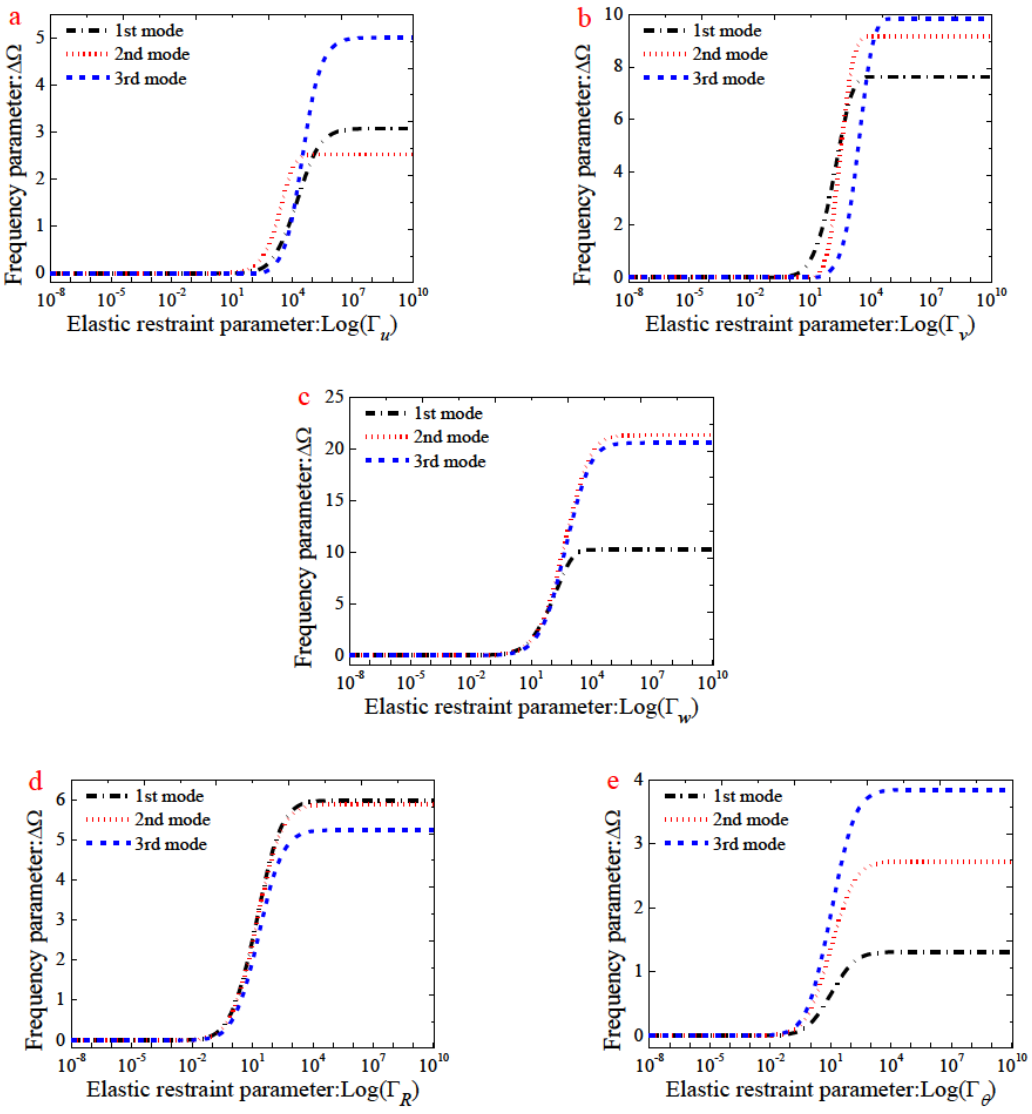

Figure 3: Variation of the frequency parameters $\Delta\Omega$ versus the elastic restraint parameters Γ_λ for a three-layered, [0°/90°/0°], symmetrically laminated annular sector plate: (a) Γ_u; (b) Γ_v; (c) Γ_w; (d) Γ_R; and (e) Γ_θ

3.3 Composite laminated annular sector plates with various boundary conditions

In this sub-section, composite laminated annular sector plates with various boundary conditions and structure parameters are investigated. First, a verification study is made to validate the accuracy and reliability of the present method. The results reported by Sharma [14] are adopted herein as the reference. And the Table 3 presents the two methods' comparison of the frequency parameters Ω for a $[0°/90°]_5$ laminated annular sector plate with different classical boundary conditions. According to the results, it is clear that the difference between the two methods is no more than 0.634% for the worst case.

Numerous new results are presented in Tables 3, 4 and 5 for composite laminated annular sector plates with a variety of boundary conditions including clamped boundary, simple-support boundary, free boundary and their combinations. These results may serve as benchmark solutions for potential readers. In Table 3, the first six non-dimension frequency Ω for four-layered, cross-ply [0°/90°/0°/90°] laminated annular sector plate subjected to as many as 8 possible classical boundary conditions are presented. The material properties and geometric dimensions used in the analysis are $\phi = \pi/2$, a/b=0.5, E_1/E_2=15. Three thickness-to-radius ratios, namely, h/b = 0.05, 0.10 and 0.2, are considered in the calculation. In addition, it also can be seen from the table that the augmentation of the thickness-to-radius makes frequency

Table 3: Frequency parameters Ω for a [0°/90°/0°/90°] laminated annular sector plate with different thickness-to- radius ratios and boundary conditions ($\phi = \pi/2$, a/b=0.5, E_1/E_2=15).

h/b	Mode	Boundary conditions							
		CCCC	SSSS	FFFF	CSCS	CFCF	CSCF	SFSF	CFFF
0.05	1	13.609	7.499	2.398	13.323	13.156	13.177	7.142	2.172
	2	15.563	9.489	2.606	14.497	13.235	13.540	7.323	2.244
	3	19.642	13.945	5.960	17.831	13.886	15.250	8.570	3.187
	4	25.343	14.039	6.730	23.248	16.180	19.215	10.058	6.034
	5	30.297	20.280	10.621	24.760	20.743	24.563	12.000	7.283
	6	31.556	20.900	12.875	29.912	24.378	25.076	12.129	10.527
0.1	1	9.337	6.401	2.212	9.066	8.905	8.920	5.013	1.990
	2	10.892	6.973	2.468	10.241	8.965	9.277	6.032	2.058
	3	13.609	8.073	5.317	12.380	9.606	10.894	6.084	2.945
	4	17.006	10.457	5.947	12.885	11.673	12.282	6.262	3.639
	5	18.566	11.301	7.687	16.414	12.191	13.901	7.314	5.408
	6	19.555	12.380	8.874	18.400	14.997	17.605	9.990	8.756
0.2	1	5.358	3.475	1.830	5.184	5.008	5.022	2.495	1.577
	2	6.342	4.510	2.119	6.152	5.061	5.393	3.023	1.619
	3	7.886	5.201	3.768	6.190	5.715	6.140	4.226	1.824
	4	9.675	5.666	4.022	7.760	6.091	6.636	4.351	2.428
	5	10.186	6.190	4.577	9.612	7.179	8.383	5.082	4.119
	6	10.686	7.352	5.531	10.075	9.036	9.958	5.273	5.598

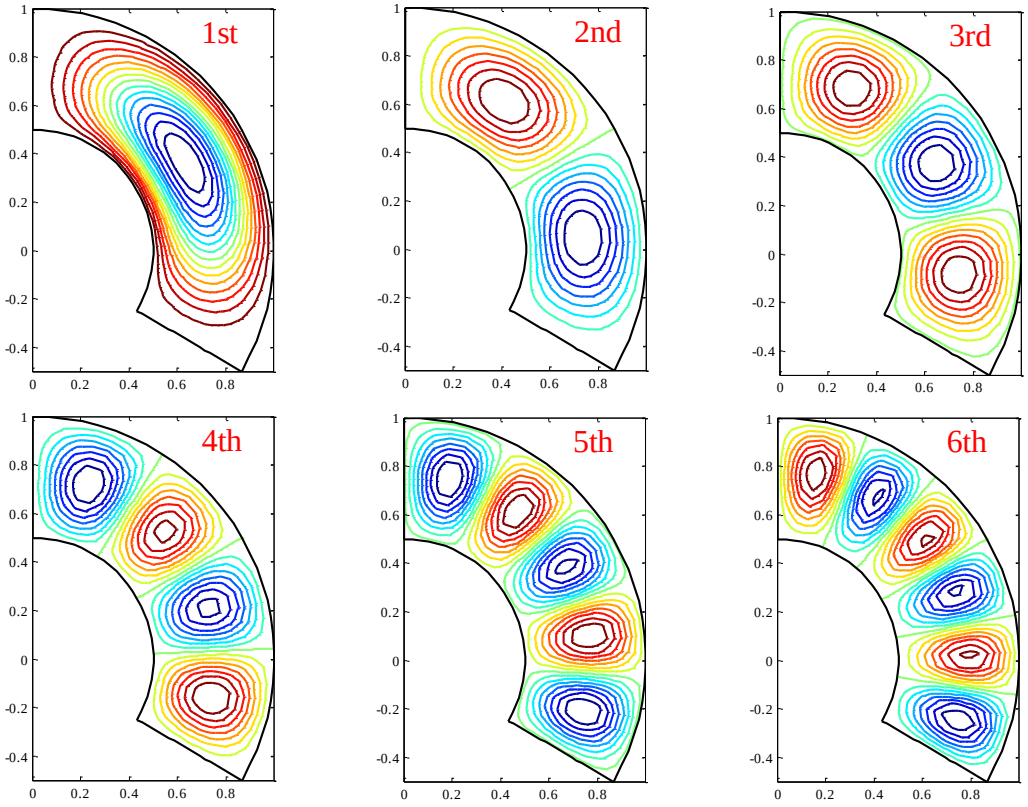

Figure 4: The lowest six mode shapes for a [0°/90°/90°/0°] laminated annular sector plate with CCCC boundary conditions(E_1/E_2=15, a/b=0.5, h/b=0.1, ϕ=2π/3)

Table 4: Frequency parameters Ω for a [0°/90°/0°/90°] laminated annular sector plate with different orthotropy ratios and boundary conditions ($\phi = \pi/2$, a/b=0.5, h/b=0.1).

E_1/E_2	Mode	Boundary conditions							
		CCCC	SSSS	FFFF	CSCS	CFCF	CSCF	SFSF	CFFF
5	1	7.832	4.748	1.751	7.657	7.477	7.509	3.767	1.369
	2	9.125	6.189	2.143	8.556	7.598	7.877	4.334	1.500
	3	11.482	6.272	3.969	10.635	8.186	9.099	4.640	2.243
	4	14.572	9.008	4.921	12.380	9.727	11.470	5.586	3.488
	5	16.508	9.978	6.104	13.679	12.032	12.199	5.797	4.029
	6	16.721	12.380	6.795	16.303	12.361	14.685	8.013	6.643
10	1	8.805	5.728	2.173	8.575	8.417	8.438	4.519	1.728
	2	10.245	6.642	2.189	9.605	8.495	8.777	5.386	1.816
	3	12.828	7.312	4.765	12.020	9.082	10.199	5.574	2.630
	4	16.125	10.281	5.489	12.380	10.904	12.255	5.869	3.593
	5	17.858	10.362	7.153	15.393	12.140	12.961	6.669	4.819
	6	18.768	12.380	8.044	17.698	13.969	16.513	9.147	7.910
20	1	9.680	6.904	2.225	9.379	9.206	9.219	5.390	2.197
	2	11.321	7.245	2.697	10.683	9.256	9.604	6.216	2.254
	3	14.128	8.664	5.741	12.380	9.967	11.391	6.594	3.213
	4	17.585	10.589	6.336	13.486	12.185	12.298	6.728	3.665
	5	19.022	12.001	8.011	17.099	12.273	14.561	7.821	5.879
	6	20.057	12.380	9.484	18.848	15.722	18.335	10.453	9.379
40	1	10.355	8.010	2.251	9.994	9.760	9.769	6.398	2.753
	2	12.193	8.150	3.317	11.670	9.795	10.292	6.729	2.787
	3	15.191	10.142	6.818	12.380	10.790	12.326	7.778	3.715
	4	18.750	10.967	7.471	14.781	12.275	12.537	7.855	4.015
	5	19.948	12.380	8.613	18.492	13.560	15.999	9.144	7.160
	6	21.088	13.645	10.908	19.755	17.316	19.563	10.775	10.817

parameters decrease. Then a moderately thick (h/b=0.1) four-layered, cross-ply [0°/90°/0°/90°] plate with various anisotropic degrees is considered. In Table 4, the first six frequency parameters Ω for the laminated annular sector plate with eight types of classical boundary conditions and six different anisotropic degrees, *i.e.*, E_1/E_2 = 5, 10, 20 and 40 are listed, respectively. The geometric dimensions of the considered plate are the same as the model used for Table 3 except $\phi = \pi/2$. From Table 4, it is shown that the frequency parameters, in general, increase as the anisotropic ratio increases. In the next example, we consider a moderately thick (h/b=0.1) four-layered, cross-ply [0°/90°/90°/0°] plate with various included angles. The first six frequency parameters Ω for the laminated annular sector plate with various classical boundary conditions and included angles, *i.e.* ϕ=60^o, 120^o, 240^o and 360^o, are presented in Table 5. The results show that the frequency parameters of the sector plates monotonically decrease with the included angles increasing. The first six of mode shapes for CCCC and CFCF laminated annular sector plates are given in Figs. 4-5.

As we all know, a variety of possible restraint conditions are usually encountered in engineering applications, but the corresponding vibration analysis is quite scarce. Therefore, the composite laminated annular sector plates subjected to general elastic restraints, are studied in the last example. The first six non-dimension frequency Ω of laminated annular sector plates with classical-elastic restraints (CE^1CE^1, CE^2CE^2, CE^3CE^3, SE^1SE^1, SE^2SE^2, SE^3SE^3, E^1FE^1F, E^2FE^2F and E^3FE^3F) and elastic boundaries ($E^1E^2E^1E^2$, $E^1E^3E^1E^3$, $E^2E^3E^3E^3$, $E^1E^1E^1E^1$, $E^2E^2E^2E^2$, $E^3E^3E^3E^3$, $E^2E^1E^2E^1$, $E^3E^1E^3E^1$and $E^3E^2E^3E^2$) are presented in Tables 6 and 7. These results may serve as benchmark solutions for potential readers. The geometric dimensions of the considered plate are the same as the model used for Table 3 except $\phi = \pi$. Three Lamination schemes, *i.e.* [0°/90°], [0°/90°/0°] and [0°/90°/90°/0°], are performed in the calculation. Compared with classical boundary conditions, the frequency

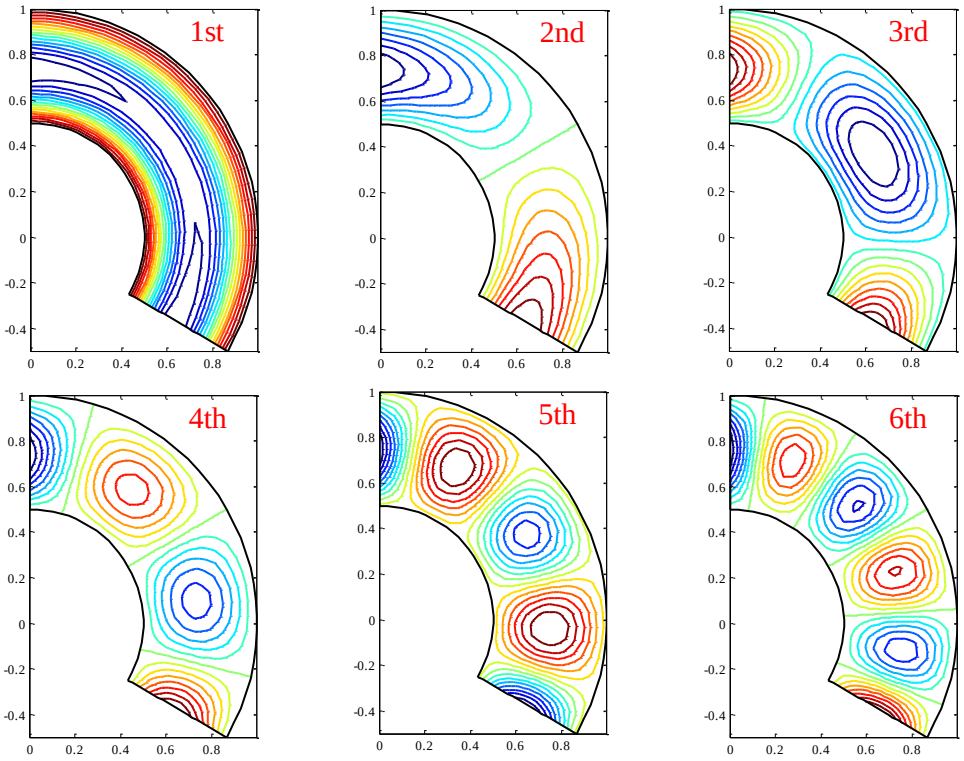

Figure 5: The lowest six mode shapes for a [0°/90°/90°/0°] laminated annular sector plate with CFCF boundary conditions(E_1/E_2=15, a/b=0.5, h/b=0.1, ϕ=2π/3)

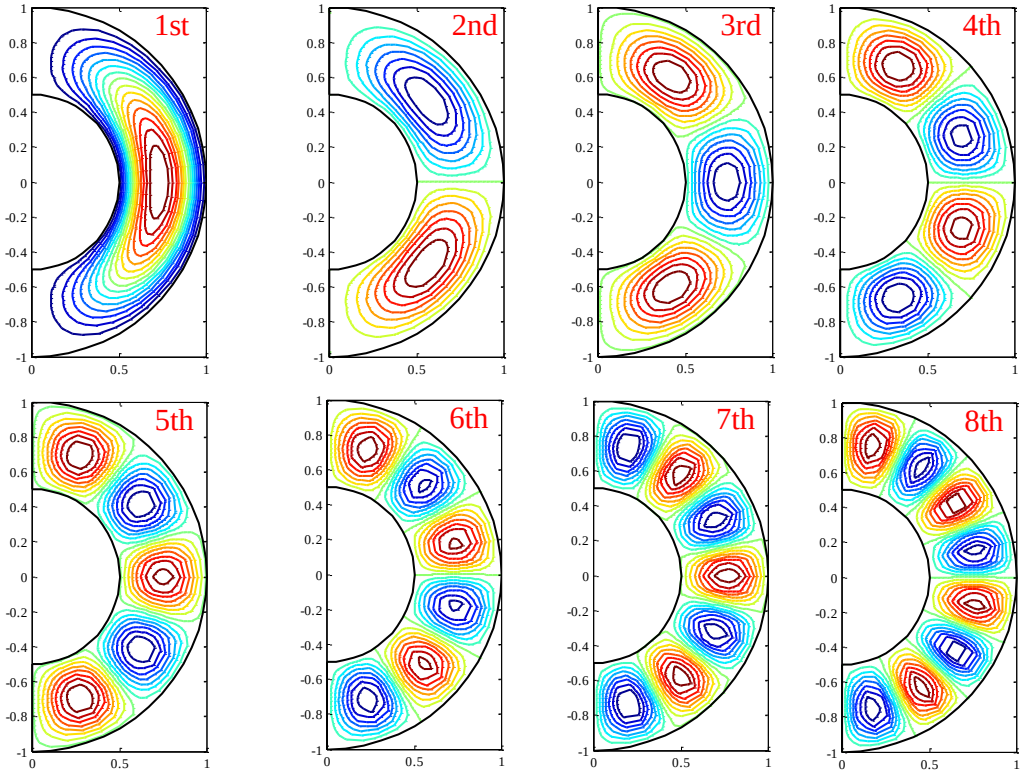

Figure 6: The lowest eight mode shapes for a [0°/90°/90°/0°] laminated annular sector plate with CE^3CE^3 boundary conditions(E_1/E_2=15, a/b=0.5, h/b=0.1, $\phi = \pi$)

Table 5: Frequency parameters Ω for a [0°/90°/90°/0°] laminated annular sector plate with different included angles and boundary conditions (E_1/E_2=15, a/b=0.5, h/b=0.1).

ϕ	Mode	Boundary conditions							
		CCCC	SSSS	FFFF	CSCS	CFCF	CSCF	SFSF	CFFF
60	1	10.374	7.802	3.320	9.857	9.573	9.598	4.144	2.522
	2	13.145	8.335	3.460	11.954	9.670	10.219	7.281	2.659
	3	17.550	10.536	7.802	12.380	10.767	12.232	7.562	3.541
	4	19.818	12.380	8.271	16.283	12.086	12.994	8.016	4.140
	5	21.773	15.325	12.943	19.552	14.184	17.743	9.231	7.915
	6	22.697	15.401	13.064	21.081	19.210	19.309	11.716	10.655
120	1	9.663	6.917	1.192	9.612	9.573	9.580	5.455	2.537
	2	10.070	7.380	1.511	9.857	9.598	9.664	5.660	2.553
	3	11.013	7.802	2.526	10.583	9.740	10.019	7.285	2.726
	4	12.549	8.335	3.615	11.955	10.221	10.912	7.356	3.367
	5	14.574	8.824	4.404	12.380	11.289	12.315	7.660	3.688
	6	16.938	10.536	5.007	13.914	12.253	12.456	8.212	4.724
240	1	9.586	6.917	0.360	9.581	9.574	9.575	5.571	2.540
	2	9.632	7.197	0.680	9.612	9.580	9.590	5.625	2.546
	3	9.743	7.309	1.105	9.692	9.604	9.635	7.207	2.555
	4	9.954	7.380	1.202	9.857	9.664	9.737	7.286	2.612
	5	10.297	7.532	1.462	10.145	9.790	9.934	7.304	2.763
	6	10.793	7.803	1.842	10.585	10.020	10.261	7.368	3.067
360	1	9.578	6.917	0.110	9.577	9.574	9.575	5.635	2.541
	2	9.593	6.981	0.288	9.588	9.576	9.581	5.639	2.543
	3	9.624	7.297	0.568	9.612	9.586	9.596	7.033	2.554
	4	9.682	7.326	0.706	9.658	9.606	9.627	7.287	2.555
	5	9.777	7.380	0.827	9.736	9.644	9.682	7.295	2.586
	6	9.921	7.458	1.063	9.857	9.709	9.771	7.322	2.655

variations of the laminated annular sector plates subjected to elastic restraints and classical-elastic restraints with different lamination schemes are more complex. Form the Table 6 and 7, it is also obvious that the lamination schemes have significant effect on the frequency of the laminated annular sector plates. Some mode shapes for CE^3CE^3, and $E^3E^3E^3E^3$ laminated annular sector plates are depicted in Figs. 6-7.

3.4 Parameters study

In a composite lamina, fibers are the principal load carrying members. By appropriately arranging the fiber directions in the layers of a laminated plate, special functional requirements can be satisfied. Owing to the practical importance, the influence of fiber orientations on the vibration characteristics of composite laminated annular sector plates is investigated in this part. In Fig. 8(a)-8(d), the variation of the lowest four frequency parameters Ω versus the included angle θ for a three-layered $[0^o/\alpha^o/0^\circ]$ laminated annular sector plate with CCCC, CFFF, CSCF and CFCF boundary conditions against the included angle θ are depicted, respectively. The geometric and material properties of the layers are a/b=0.5, h/b=0.1, $\phi = \pi/2$ and E_1/E_2=15. Many interesting characteristics can be observed from the figures. Firstly, all the figures are symmetrical about α= 90^o. Second, from the Fig. 2(a)–2(d), it can be shown that all the mode frequency parameters of the plate decrease with the included angle α increasing. And there is little variation in frequency parameters of the 4th modes. From Fig. 2(b), the results show that the 4th mode frequency parameter first remains unchanged and then declines.

As the last case of this section, the influence of the number of layers on the fundamental frequency parameters of a laminated annular sector is investigated. In Figs. 9 and 10, the variation of the lowest four frequency parameters Ω of a $[0^o/\alpha^o]_n$ (where n=1 means a two-layered plate; n=2 means a four-layered plate, *i.e.*, $[0^o/\alpha^o/0^o/\alpha^o]$, and so forth) layered plate with SFSF and FSFS boundary condi-

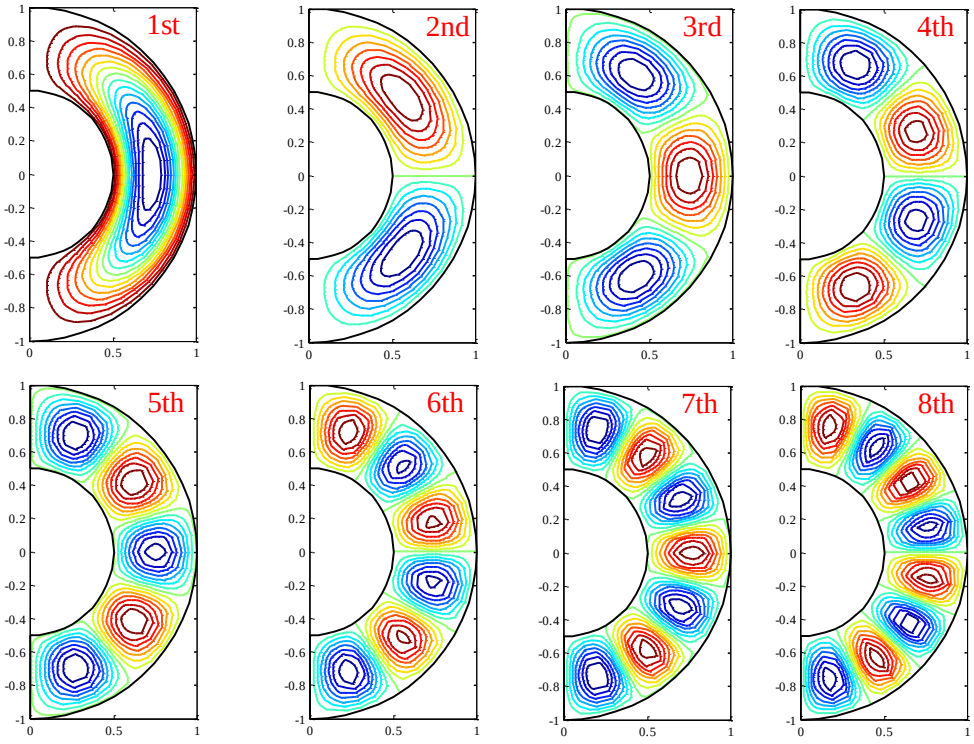

Figure 7: The lowest eight mode shapes for a [0°/90°/90°/0°] laminated annular sector plate with $E^3E^3E^3E^3$ boundary conditions(E_1/E_2=15, a/b=0.5, h/b=0.1, $\phi = \pi$)

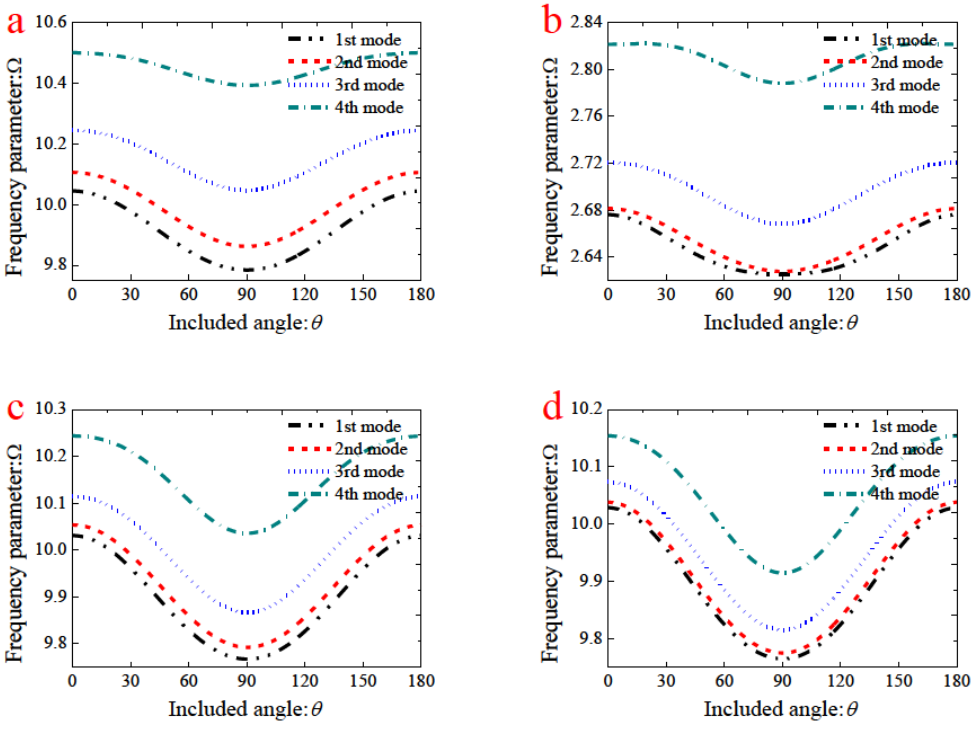

Figure 8: Variation of the frequency parameters Ω versus the included angle θ for a three-layered [$0^o/\theta^o/0^\circ$] laminated annular sector plate with different boundary conditions: (a) CCCC; (b) CFFF; (c) CSCF; and (d) CFCF.

Table 6: Frequency parameters Ω for laminated annular sector plate with different lamination schemes and classical-elastic boundary conditions (E_1/E_2=15, a/b=0.5, h/b=0.1, $\phi = \pi$).

Lamination schemes	Mode	Boundary conditions								
		CE^1CE^1	CE^2CE^2	CE^3CE^3	SE^1SE^1	SE^2SE^2	SE^3SE^3	E^1FE^1F	E^2FE^2F	E^3FE^3F
0°/90°	1	7.962	7.963	7.964	5.129	5.137	5.138	1.477	1.468	7.285
	2	8.107	8.060	8.104	5.334	5.325	5.374	1.484	1.704	7.286
	3	8.494	8.249	8.471	5.490	5.705	5.944	1.653	2.316	7.403
	4	9.189	8.580	9.137	5.761	6.292	6.889	2.919	3.174	7.663
	5	10.199	9.140	10.121	6.030	7.112	7.757	5.133	4.232	8.181
	6	11.484	10.031	11.384	6.948	7.786	7.952	7.747	5.335	9.019
0°/90°/0°	1	9.784	9.779	9.783	5.217	7.445	7.445	1.478	1.476	8.772
	2	9.862	9.828	9.859	5.572	7.449	7.449	1.484	1.704	8.789
	3	10.047	9.913	10.038	6.943	7.535	7.543	1.653	2.274	8.853
	4	10.393	10.063	10.374	7.544	7.651	7.696	2.750	3.042	8.993
	5	10.944	10.328	10.911	7.701	7.850	8.001	4.934	3.949	9.259
	6	11.719	10.786	11.672	8.015	8.157	8.508	7.683	4.981	9.705
0°/90°/90°/0°	1	8.962	8.946	8.956	5.519	6.198	6.209	1.477	1.473	8.034
	2	9.177	9.037	9.149	5.875	6.406	6.522	1.484	1.713	8.049
	3	9.691	9.210	9.626	6.215	6.767	7.215	1.653	2.380	8.158
	4	10.565	9.610	10.464	6.559	7.395	7.822	2.945	3.401	8.479
	5	11.777	10.366	11.654	7.304	7.838	8.017	5.174	4.704	9.162
	6	12.330	11.518	13.129	7.417	8.010	8.348	8.005	6.186	10.263

Table 7: Frequency parameters Ω for laminated annular sector plate with different lamination schemes and elastic boundary conditions (E_1/E_2=15, a/b=0.5, h/b=0.1, $\phi = \pi$).

Lamination schemes	Mode	Boundary conditions								
		$E^1E^2E^1E^2$	$E^1E^3E^1E^3$	$E^2E^3E^3E^3$	$E^1E^1E^1E^1$	$E^2E^2E^2E^2$	$E^3E^3E^3E^3$	$E^2E^1E^2E^1$	$E^3E^1E^3E^1$	$E^3E^2E^3E^2$
0°/90°	1	3.202	3.189	1.791	1.613	1.584	7.362	1.801	7.360	7.360
	2	5.226	5.207	2.568	1.628	1.936	7.527	2.606	7.531	7.476
	3	7.950	7.951	3.602	1.932	2.574	7.938	3.666	7.964	7.700
	4	8.010	8.032	4.817	3.189	3.490	8.663	4.901	8.719	8.079
	5	8.095	8.090	5.766	5.281	4.630	9.711	5.681	9.792	8.693
	6	8.221	8.446	6.181	7.834	5.710	11.034	6.278	11.136	9.644
0°/90°/0°	1	3.133	3.133	1.752	1.612	1.583	8.801	1.757	8.801	8.795
	2	5.001	5.001	2.429	1.627	1.919	8.904	2.446	8.908	8.869
	3	7.819	7.819	3.331	1.930	2.487	9.129	3.361	9.140	8.998
	4	8.318	8.318	4.381	3.041	3.263	9.531	4.423	9.552	9.208
	5	9.779	9.783	5.546	5.087	4.214	10.147	5.598	10.183	9.534
	6	9.828	9.859	6.809	7.768	5.311	10.994	6.870	11.045	10.066
0°/90°/90°/0°	1	3.215	3.213	1.828	1.613	1.592	8.092	1.859	8.099	8.082
	2	5.254	5.249	2.743	1.629	1.955	8.316	2.828	8.347	8.204
	3	8.173	8.165	3.993	1.932	2.687	8.851	4.116	8.921	8.425
	4	8.943	8.954	5.435	3.212	3.820	9.769	5.577	9.877	8.884
	5	9.034	9.145	6.820	5.316	5.225	11.047	6.815	11.175	9.710
	6	9.205	9.304	7.006	8.089	6.727	12.604	7.153	12.330	10.945

Table 8: Comparison of the first six frequency parameters $\Omega=\omega b^2(\rho h/D)^{1/2}$ for a isotropic annular sector plates with h/b = 0.001(thin plate), a/b=0.2 and $\phi = \pi/3$.

Line supports	Boundary conditions		Mode number					
			1	2	3	4	5	6
None	SSSS		40.31	97.52	98.00	177.6136	179.8623	183.9804
	FSFS		62.50	109.5	110.7227	163.9777	164.7611	167.7842
r_1=$R/2$	SSSS	present	85.40	127.7	142.6	193.7	279.6	285.0
		Ref [16]	85.41	127.9	142.6	194	279.8	285.1
		Error(%)	0.02	0.17	0.01	0.16	0.06	0.03
	FSFS	present	21.34	51.09	103.4	109.3	141.0	173.7
		Ref[16]	21.34	51.11	103.5	109.3	141.3	174
		Error(%)	0.01	0.03	0.06	0.01	0.24	0.19
r_1=$R/2$, θ_1=$\phi/2$	SSSS	present	127.7	148.2	285.0	285.7	330.9	336.3
		FEM	127.8	148.3	285.3	286.1	331.1	336.4
		Error(%)	0.10	0.09	0.10	0.13	0.06	0.04
	FSFS	present	51.09	73.51	173.7	176.5	192.8	220.3
		FEM	51.21	73.64	173.8	176.9	193.1	220.8
		Error(%)	0.23	0.17	0.07	0.20	0.17	0.21

tions against the number of layers n are depicted, respectively. Four lamination schemes, namely, $\alpha = 30^o, 45^o, 60^o$ and 90^o are considered in the investigation. The layers of the laminated annular sector plate are of equal thickness and made from the same material with following proprieties: E_1/E_2=15. The geometric parameters of the plate are a/b=2, h/a=0.1. As clearly observed from Figs. 3 and 4, the frequency parameters of the plate increases rapidly and may reach their crest around n = 5 (10 layer), and beyond this range, the frequency parameters remain unchanged. In such a case, the laminated annular sector can be treated as an orthotropic annular sector plate.

3.5 Composite laminated annular sector plates with internal line/arc supports

In the engineering application, the composite laminated annular sector plates are often restrained by internal radial lines and circumferential arc supports to reduce the magnitude of dynamic and static stresses and displacements of the structure or to satisfy special architectural and functional requirements. The study of the vibrations of moderately thick, composite laminated annular sector plates is an important aspect in the successful applications of these structures. However, to the best of the authors' knowledge, no researches dealing with the free vibration characteristics of the composite laminated annular sector with general boundary conditions, internal radial line and circumferential supports have been reported. Thus, in this part, the present formulations are applied to investigate the free vibration behaviors of composite laminated annular sector plates with internal line/arc supports and arbitrary boundary conditions. As shown in Fig. 7, the composite laminated annular sector plates is restrained by arbitrary internal radial line and circumferential arc supports. r_i and θ_j represent the position of the ith and jth internal radial line and circumferential arc supports along the r- and θ-directions, respectively. The displacement fields in the position of the line support satisfy $w(r_i, \theta, t) = 0$ and $w(r, \theta_j, t) = 0$. This condition can be readily obtained by introducing a group of continuously distributed linear springs at the location of each line/arc support and setting the stiffnesses of these springs equal to infinite (which is represented by a very large number, $10^8 D$). Thus, the potential energy (P_{rals}) stored in these springs is

$$P_{rals} = \frac{1}{2}\int_0^{\phi}\left\{\sum_{i=1}^{N_i} k_{ri}^i w(r_i,\theta,t)^2 (r_i + a)\right\} d\theta + \frac{1}{2}\int_0^{R}\left\{\sum_{j=1}^{M_i} k_{\theta j}^i w(r,\theta_i,t)^2\right\} ds$$

where M_j and N_i are the amount of radial line and circumferential arc supports in the r and θ directions. k_{ri}^i and

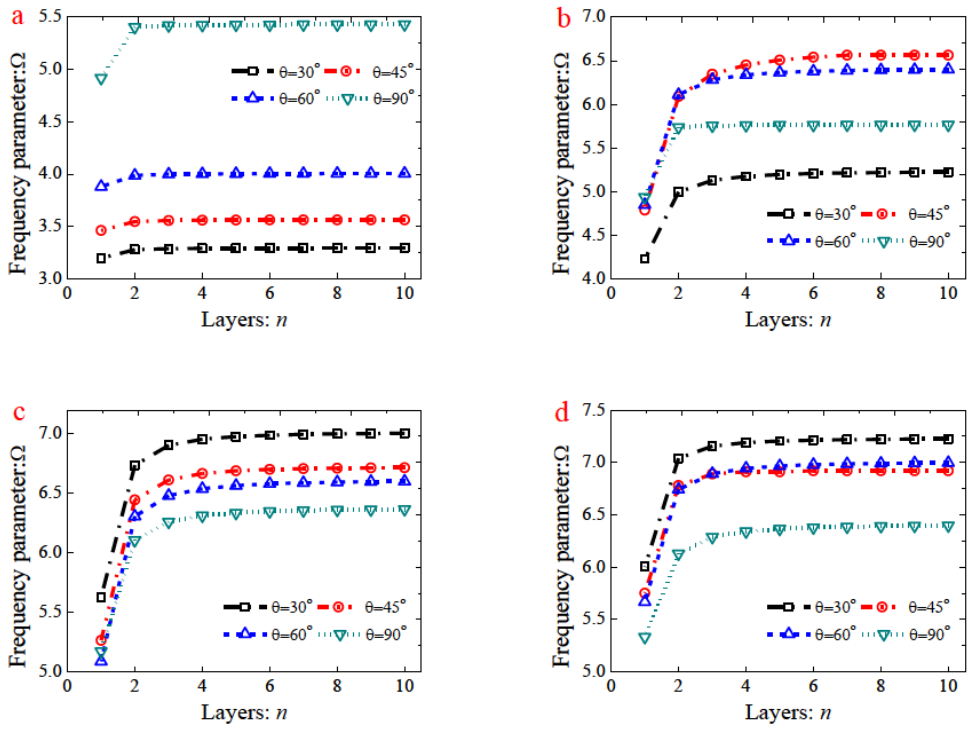

Figure 9: Variation of the frequency parameters Ω number of layers n for a $[0^o/\theta^o]_n$ layered annular sector plate with SFSF boundary conditions: (a) 1st mode; (b) 2nd mode; (c) 3rd mode; and (d) 4th mode.

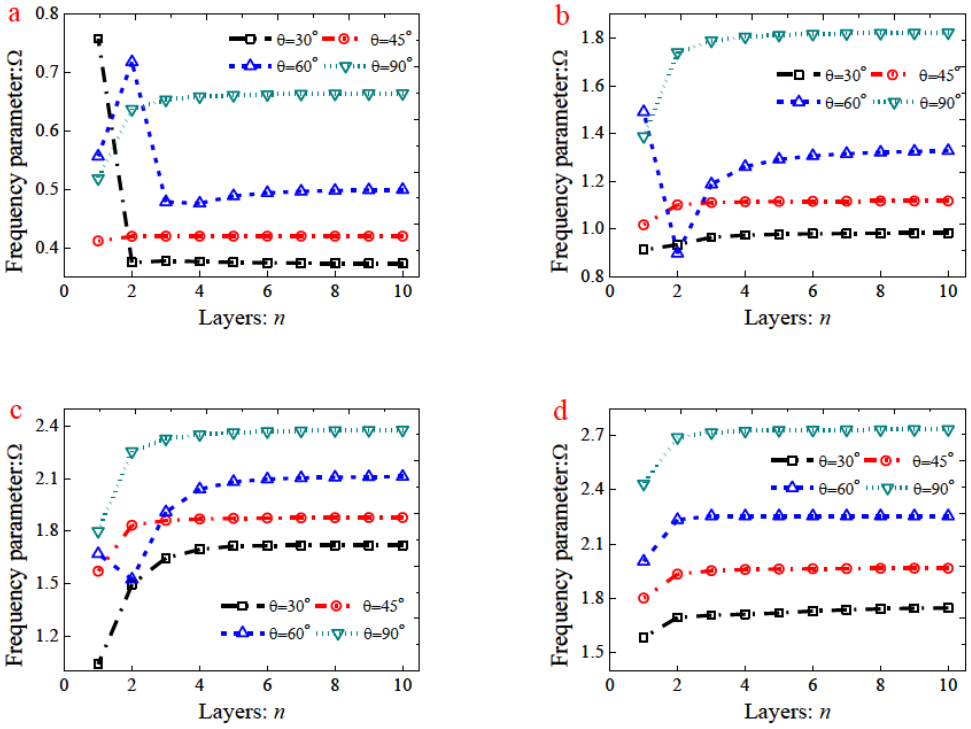

Figure 10: Variation of the frequency parameters Ω number of layers n for a $[0^o/\theta^o]_n$ layered annular sector plate with FSFS boundary conditions: (a) 1st mode; (b) 2nd mode; (c) 3rd mode; and (d) 4th mode.

Table 9: The first five frequency parameters Ω for a four-layered, [90°/0°/0°/90°] annular sector plate with different boundary conditions and various line supports (a/b=0.2, h/b=0.1, $\phi = \pi$, E_1/E_2=15).

Line supports	Mode	Boundary conditions							
		CCCC	FFFF	SSSS	CFCF	$E^1E^1E^1E^1$	$E^2E^2E^2E^2$	$E^3E^3E^3E^3$	$CE^1E^2E^3$
$r_1=R/2$	1	22.490	3.293	17.723	21.489	22.490	7.783	21.428	8.445
	2	24.310	3.404	19.040	21.546	24.310	8.799	23.131	9.620
	3	26.427	4.234	21.112	22.989	26.427	9.991	25.208	11.982
	4	27.692	5.675	23.623	25.148	27.692	12.052	26.598	15.344
	5	29.036	8.113	23.992	26.910	29.036	12.622	27.822	19.370
	6	30.645	8.930	26.758	26.961	30.645	15.154	29.433	23.793
$r_1=R/3$, $r_2=2R/3$	1	36.242	8.340	32.998	35.469	36.242	14.520	35.627	14.606
	2	37.655	8.397	33.881	35.583	37.655	15.058	36.934	15.370
	3	39.695	8.741	35.287	36.784	39.695	15.942	38.811	16.927
	4	42.173	9.392	37.215	38.659	42.173	17.406	41.093	19.337
	5	43.001	11.422	37.900	41.025	43.001	19.591	41.585	22.478
	6	44.811	13.755	39.659	42.091	44.811	19.835	43.463	26.165
$r_1=R/2$, $\theta_1=\phi/2$	1	24.310	3.404	19.040	21.546	24.310	8.799	23.131	9.605
	2	24.992	4.003	19.598	21.912	24.992	9.221	23.782	10.426
	3	29.036	5.675	23.992	25.148	29.036	12.052	27.822	15.312
	4	29.980	7.128	25.010	25.788	29.980	13.030	28.774	16.677
	5	30.645	9.986	26.758	26.961	30.645	16.611	29.433	23.770
	6	32.256	11.597	28.538	27.277	32.256	17.945	31.052	25.290
$r_1=R/3$, $\theta_1=\phi/2$, $r_2=2R/3$	1	37.655	8.340	33.881	35.583	37.655	15.058	36.934	15.362
	2	38.149	8.463	34.167	35.748	38.149	15.278	37.379	15.779
	3	42.173	9.392	37.215	38.659	42.173	17.406	41.093	19.315
	4	42.878	10.348	37.799	39.200	42.878	17.999	41.757	20.286
	5	44.811	14.588	40.256	42.220	44.811	22.611	43.463	26.146
	6	45.321	15.712	41.078	42.491	45.321	23.663	44.039	27.430

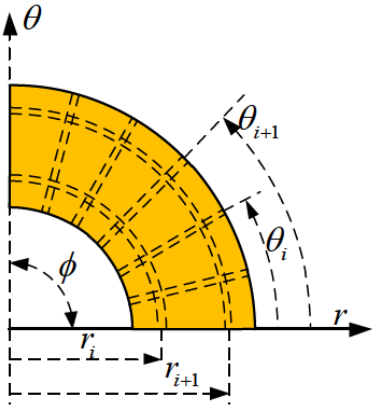

Figure 11: Schematic diagram of a laminated annular sector plate with arbitrary internal radial line and circumferential arc supports.

$k^i_{\theta j}$ denote the corresponding radial line and circumferential arc supported springs distributed at r=r_i and $\theta = \theta_j$. For an annular sector plate with elastic restraints on the edges as well as the internal radial line and circumferential arc supports, the potential energy P_{rals} stored in the line/arc supported springs should be considered as part of the Lagrangian energy function (Eq. (21)). Adopting the Rayleigh-Ritz rule, the characteristic equation of the structure can be obtained easily.

Table 8 presents the first six frequency parameters Ω=ωb^2 $(\rho h/D)^{1/2}$ for a isotropic annular sector plate with h/b = 0.001(thin plate), a/b=0.2 and $\phi = \pi/3$, which can be used to check the correctness of using the present formulations to study the titled vibration problem. Two different classical boundary conditions, *i.e.*, SSSS and FSFS are considered in the comparison. The results of the annular

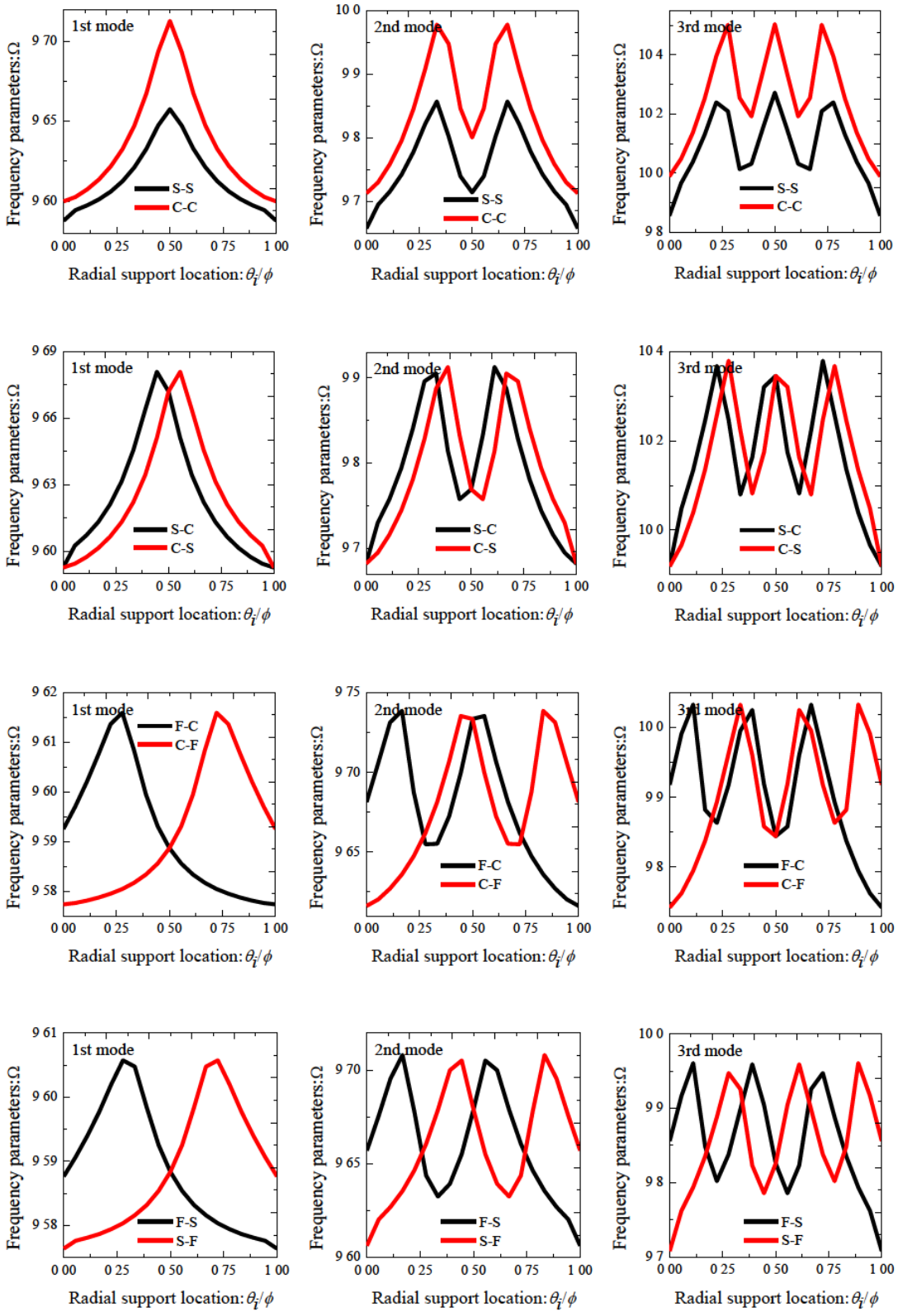

Figure 12: Variation of the frequency parameters Ω versus the radial support locations for a [0°/90°/90°/0°] laminated annular sector plate with a θ direction internal radial support (E_1/E_2=15, a/b=0.5, h/b=0.1, $\phi = \pi$)

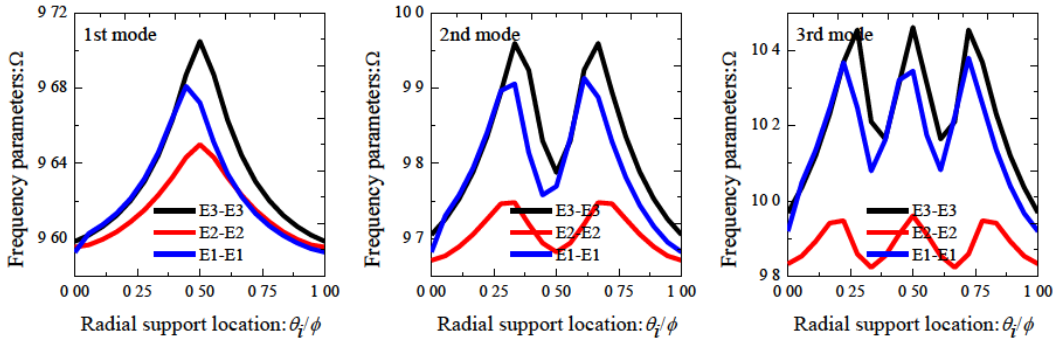

Figure 12: Variation of the frequency parameters Ω versus the radial support locations for a [0°/90°/90°/0°] laminated annular sector plate with a θ direction internal radial support (E_1/E_2=15, a/b=0.5, h/b=0.1, $\phi = \pi$)

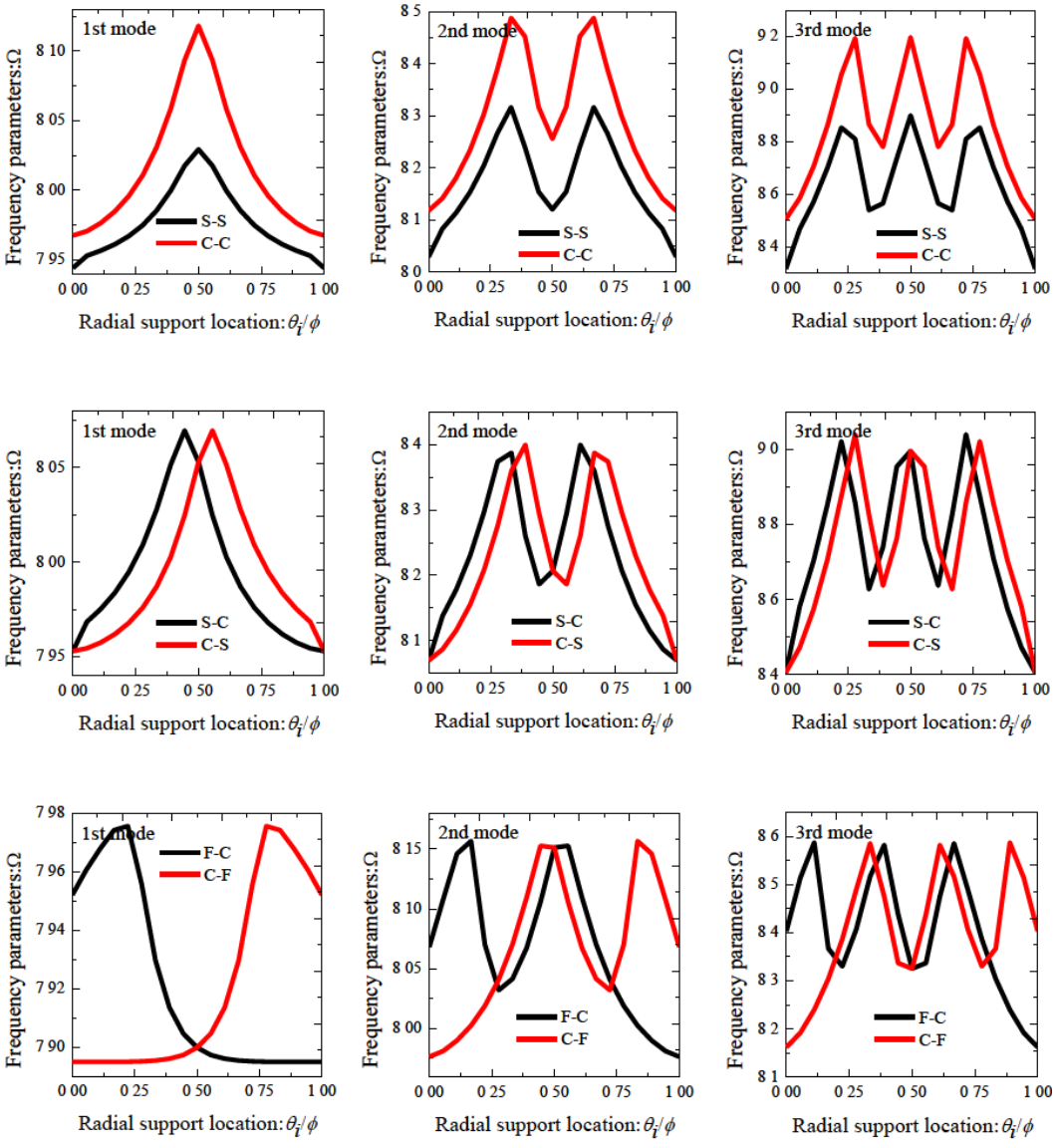

Figure 13: Variation of the frequency parameters Ω versus the radial support locations for a [0°/90°] laminated annular sector plate with a θ direction internal radial support (E_1/E_2=15, a/b=0.5, h/b=0.1, $\phi = \pi$)

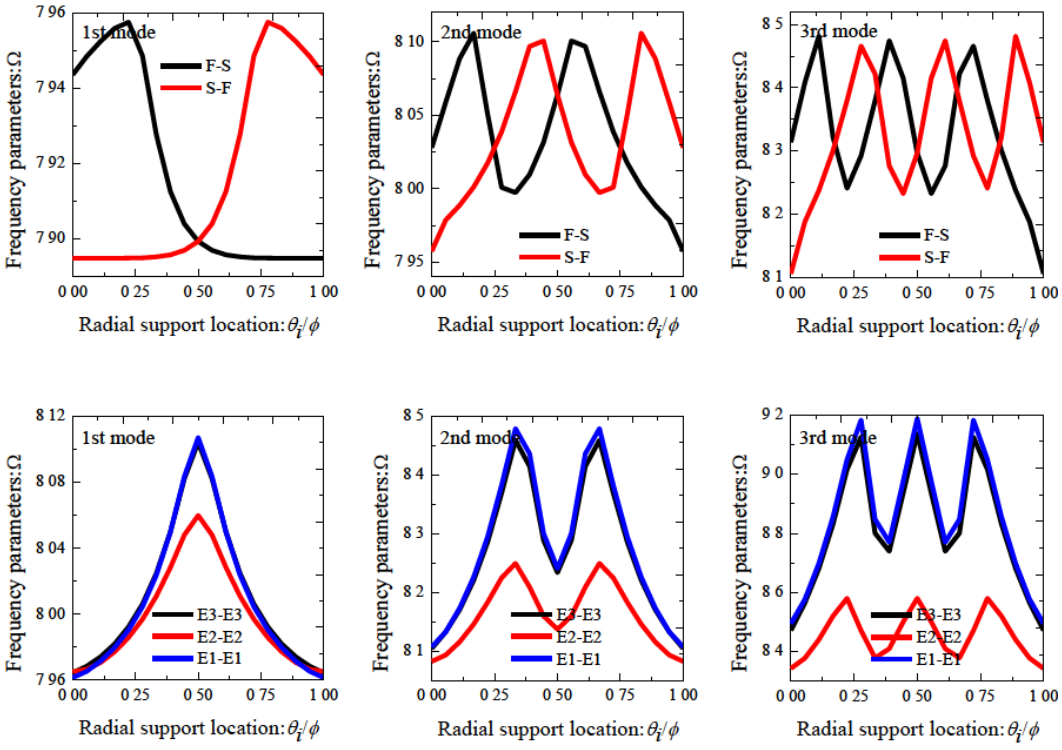

Figure 13: Variation of the frequency parameters Ω versus the radial support locations for a [0°/90°] laminated annular sector plate with a θ direction internal radial support (E_1/E_2=15, a/b=0.5, h/b=0.1, $\phi = \pi$)

plate without line/arc support are given in the table to be compared with those of the supported plate, which aims to stressing the effect of the line/arc supports. Benchmark results given by Liew *et al.* [5] based on MPT and obtained by the ABAQUS based on FEA method are also presented. According to the table, the good agreement between the results can be observed, where the discrepancy of the worst case does not exceed 0.24%. Besides, it also can be seen that the introducing of the line/arc supports can increase the plate frequency. Then, the influence of the locations of internal radial line and circumferential arc supports on the frequency of a four-layered, cross-ply [0°/90°/90°/0°], symmetrically laminated annular sector is investigated. The sector plate parameters are given below as h/b=0.1, a/b=0.5, $\phi = \pi$, E_1/E_2=15. For simplicity, only a radial line support along θ direction (θ_1) is considered in the analysis. In Fig. 12, variation of the lowest three mode frequency parameters Ω of the considered sector plate with symmetrically lamination schemes ([0°/90°/90°/0°]) against the radial line support location parameter θ_1/ϕ is depicted. Eleven types of edge conditions used in the investigation are: C-C, S-S, F-C, C-F, F-S, S-F, S-C, C-S, E^1-E^1, E^2-E^2, E^3-E^3. It is obvious that the frequency parameters of the sector plate significantly are affected by the position of the radial line support, and this effect varies with the edge conditions. And for different modes, the effects of radial line support location are quite different. For the sake of completeness, variation of the lowest three mode frequency parameters Ω of the considered sector plate with unsymmetrically lamination schemes ([0°/90°]) against the radial line support location parameter θ_1/ϕ are presented in Fig. 13. Comparing Fig. 12 with Fig. 13, we can see that the influence of the line/arc support location on the frequency parameters varies with lamination schemes and boundary conditions.

Since the vibration results for internal radial line and circumferential arc supported moderately thick composite laminated annular sector plates with arbitrary boundary conditions are very limited in the literature, some new results are calculated here, which can be used for benchmark results by researchers as well as reference datum for practicing engineers. In Table 9, The first six frequency parameters Ω of the considered laminated annular sector plate with [90°/0°/0°/90°] lamination scheme and subjected to as many as 8 possible boundary conditions are presented. The sector plate is with the following proprieties: a/b=0.2, h/b=0.1, $\phi = \pi$, $E1/E2$=15. Four different line/arc support conditions are considered in the calculation. In addition, the first four mode shapes of the sector plate with CFCF boundary condition presented in Ta-

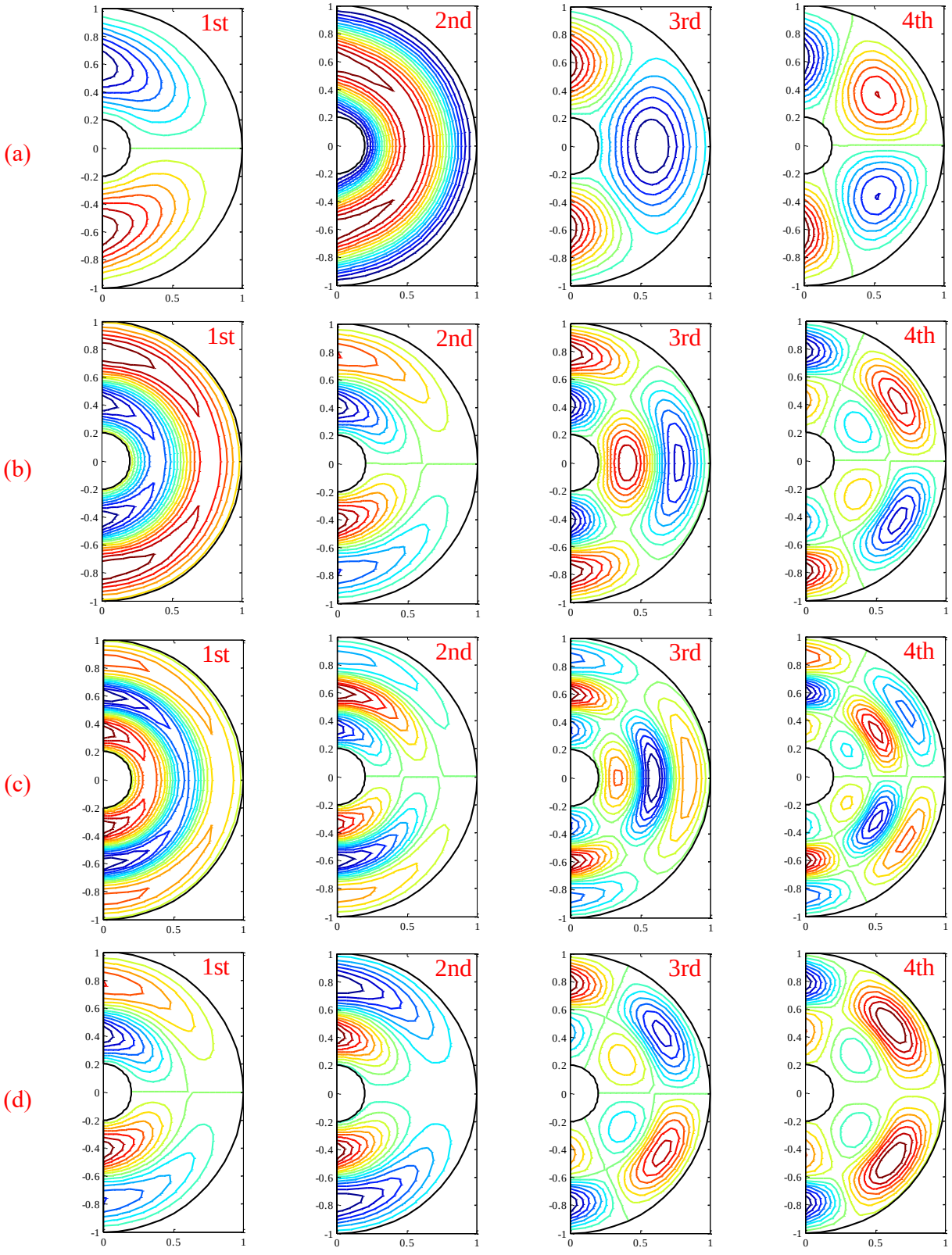

Figure 14: The lowest four mode shapes for a CFCF laminate annular sector plate with various line supports:(a) None; (b) $r_1=R/2$; (c) $r_1=R/3$, $r_2=2R/3$; (d) $r_1=R/2$, $\theta_1=\phi/2$;(e) $r_1=R/3$,$\theta_1=\phi/2$,$r_2=2R/3$.

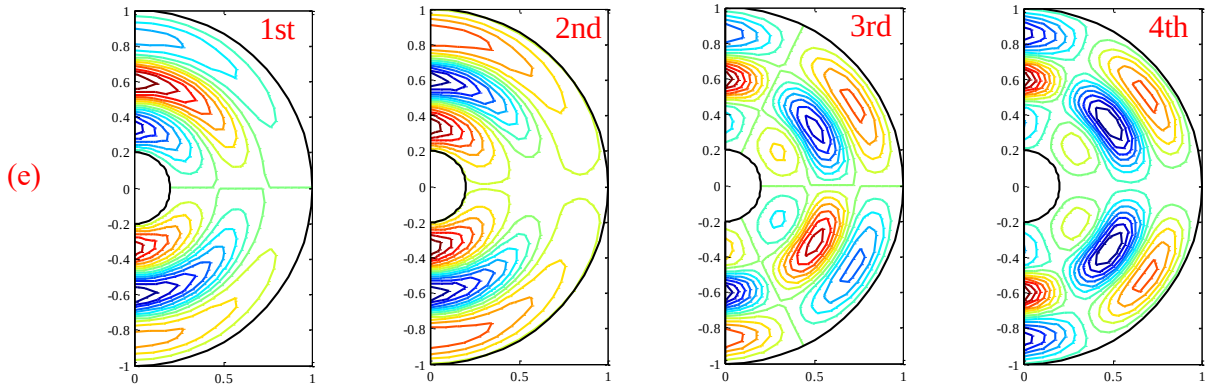

Figure 14: The lowest four mode shapes for a CFCF laminate annular sector plate with various line supports:(a) None; (b) r_1=R/2; (c) r_1=R/3, r_2=2R/3; (d) r_1=R/2, θ_1=ϕ/2;(e) r_1=R/3,θ_1=ϕ/2,r_2=2R/3.

ble 9 are also given in Fig. 14, which can improve the understanding of the vibration characteristics.

4 Conclusions

In this investigation, a modified Fourier solution based on the first-order shear deformation theory is applied to solve the free vibration problems of moderately thick composite laminated annular sector plates with general boundary conditions, internal radial line and circumferential arc supports. Each of displacements and rotations of composite laminated annular sector plate with any type of boundary conditions, is expressed by a modified Fourier series, in which auxiliary polynomial functions are supplemented to a standard Fourier cosine series. The introduction of these auxiliary functions contributes to eliminating the relevant discontinuities of the displacement function and its derivatives at the edges and accelerating the convergence of series. Raleigh-Ritz procedure is used to obtain the exact solution based on the energy functions of the laminated annular sector plate. The excellent accuracy and reliability of the current solutions are confirmed by comparing the present results with those available in the literatures, and numerous new results for composite laminated annular sector plate with various classical cases, classical-elastic restraints, elastic boundary conditions, internal radial line and circumferential arc supports are presented, which can serve as the benchmark solution for other computational techniques in the future research. The effects of elastic restraint parameters, layout orientations, number of layers and locations of line/arc supports are also investigated and reported.

Acknowledgement: The authors gratefully acknowledge the financial support from the National Natural Science Foundation China (No.51209052), Heilongjiang Province Natural Science Foundation (QC2011C013), Fundamental Research Funds for the Central Universities(HEUCFD1515), High Technology Ship Funds of Minersity of Industry and Information Technology of P.R. China, Opening Funds of State Key Laboratory of Ocean Engineering of Shanghai Jiaotong University (No.1307), funded by China Postdoctoral Science Foundation (NO.2014M552661).

References

[1] Leissa, A.W., Vibration of plates. 1973, Washington DC: U. S. Government Printing Office.
[2] Qatu, M.S., Vibration of laminated shells and plates. 2004: Elsevier.
[3] Reddy, J.N., Mechanics of laminated composite plates and shells: theory and analysis. 2004: CRC press.
[4] Carrera, E., S. Brischetto, and P. Nali, Plates and shells for smart structures: classical and advanced theories for modeling and analysis. Vol. 36. 2011: John Wiley & Sons.
[5] Hosseini-Hashemi, S., *et al.*, Differential quadrature analysis of functionally graded circular and annular sector plates on elastic foundation. Materials & Design, 2010. 31(4): p. 1871-1880.
[6] Hosseini-Hashemi, S., H.R.D. Taher, and H. Akhavan, Vibration analysis of radially FGM sectorial plates of variable thickness on elastic foundations. Composite Structures, 2010. 92(7): p. 1734-1743.
[7] Aghelinejad, M., *et al.*, Nonlinear Thermomechanical Post-Buckling Analysis of Thin Functionally Graded Annular Plates Based on Von-Karman's Plate Theory. Mechanics of Advanced Materials and Structures, 2011. 18(5): p. 319-326.
[8] Mirtalaie, S. and M. Hajabasi, Free vibration analysis of functionally graded thin annular sector plates using the differential quadrature method. Proceedings of the Institution of Mechanical Engineers, Part C: Journal of Mechanical Engineering Science, 2011. 225(3): p. 568-583.

[9] Zhou, Z., *et al.*, Natural vibration of circular and annular thin plates by Hamiltonian approach. Journal of Sound and Vibration, 2011. 330(5): p. 1005-1017.
[10] Baferani, A.H., A. Saidi, and E. Jomehzadeh, Exact analytical solution for free vibration of functionally graded thin annular sector plates resting on elastic foundation. Journal of Vibration and Control, 2012. 18(2): p. 246-267.
[11] Jomehzadeh, E., A. Saidi, and S. Atashipour, An analytical approach for stress analysis of functionally graded annular sector plates. Materials & Design, 2009. 30(9): p. 3679-3685.
[12] Saidi, A. and A.H. Baferani, Thermal buckling analysis of moderately thick functionally graded annular sector plates. Composite Structures, 2010. 92(7): p. 1744-1752.
[13] Malekzadeh, P., M.G. Haghighi, and M. Atashi, Free vibration analysis of elastically supported functionally graded annular plates subjected to thermal environment. Meccanica, 2011. 46(5): p. 893-913.
[14] Saidi, A., A.H. Baferani, and E. Jomehzadeh, Benchmark solution for free vibration of functionally graded moderately thick annular sector plates. Acta mechanica, 2011. 219(3-4): p. 309-335.
[15] Mousavi, S.M. and M. Tahani, Analytical solution for bending of moderately thick radially functionally graded sector plates with general boundary conditions using multi-term extended Kantorovich method. Composites Part B: Engineering, 2012. 43(3): p. 1405-1416.
[16] Liew, K., S. Kitipornchai, and Y. Xiang, Vibration of annular sector Mindlin plates with internal radial line and circumferential arc supports. Journal of sound and vibration, 1995. 183(3): p. 401-419.
[17] Salehi, M. and A. Sobhani, Elastic linear and non-linear analysis of fiber-reinforced symmetrically laminated sector Mindlin plate. Composite structures, 2004. 65(1): p. 65-79.
[18] Sharma, A., H. Sharda, and Y. Nath, Stability and vibration of thick laminated composite sector plates. Journal of sound and vibration, 2005. 287(1): p. 1-23.
[19] Houmat, A., Large amplitude free vibration of shear deformable laminated composite annular sector plates by a sector p-element. International Journal of Non-Linear Mechanics, 2008. 43(9): p. 834-843.
[20] Andakhshideh, A., S. Maleki, and M. Aghdam, Non-linear bending analysis of laminated sector plates using generalized differential quadrature. Composite Structures, 2010. 92(9): p. 2258-2264.
[21] Maleki, S. and M. Tahani, Bending analysis of laminated sector plates with polar and rectilinear orthotropy. European Journal of Mechanics-A/Solids, 2013. 40: p. 84-96.
[22] Golmakani, M. and M. Mehrabian, Nonlinear bending analysis of ring-stiffened circular and annular general angle-ply laminated plates with various boundary conditions. Mechanics Research Communications, 2014. 59: p. 42-50.
[23] Sharma, A., Free vibration of moderately thick antisymmetric laminated annular sector plates with elastic edge constraints. International Journal of Mechanical Sciences, 2014. 83: p. 124-132.
[24] Hashemi, S.H., M. Es'haghi, and M. Karimi, Closed-form vibration analysis of thick annular functionally graded plates with integrated piezoelectric layers. International Journal of Mechanical Sciences, 2010. 52(3): p. 410-428.
[25] Golmakani, M. and M. Kadkhodayan, Nonlinear bending analysis of annular FGM plates using higher-order shear deformation plate theories. Composite Structures, 2011. 93(2): p. 973-982.
[26] Alipour, M. and M. Shariyat, Analytical stress analysis of annular FGM sandwich plates with non-uniform shear and normal tractions, employing a zigzag-elasticity plate theory. Aerospace Science and Technology, 2014. 32(1): p. 235-259.
[27] Asemi, K., M. Salehi, and M. Akhlaghi, Post-buckling analysis of FGM annular sector plates based on three dimensional elasticity graded finite elements. International Journal of Non-Linear Mechanics, 2014. 67: p. 164-177.
[28] Srinivasan, R. and V. Thiruvenkatachari, Free vibration analysis of laminated annular sector plates. Journal of sound and vibration, 1986. 109(1): p. 89-96.
[29] Ding, H.-J. and R.-Q. Xu, Free axisymmetric vibration of laminated transversely isotropic annular plates. Journal of sound and vibration, 2000. 230(5): p. 1031-1044.
[30] Xu, R., Three-dimensional exact solutions for the free vibration of laminated transversely isotropic circular, annular and sectorial plates with unusual boundary conditions. Archive of Applied Mechanics, 2008. 78(7): p. 543-558.
[31] Malekzadeh, P., Three-dimensional free vibration analysis of thick laminated annular sector plates using a hybrid method. Composite Structures, 2009. 90(4): p. 428-437.
[32] Malekzadeh, P., M.G. Haghighi, and M. Gholami, Dynamic response of thick laminated annular sector plates subjected to moving load. Composite Structures, 2010. 92(1): p. 155-163.
[33] Fantuzzi, N., *et al.*, Stability and accuracy of three Fourier expansion-based strong form finite elements for the free vibration analysis of laminated composite plates. International Journal for Numerical Methods in Engineering, 2017.
[34] Li, W.L., Free vibrations of beams with general boundary conditions. Journal of Sound and Vibration, 2000. 237(4): p. 709-725.
[35] Li, W.L., Comparison of Fourier sine and cosine series expansions for beams with arbitrary boundary conditions. Journal of Sound and Vibration, 2002. 255(1): p. 185-194.
[36] Du, J., *et al.*, An analytical method for the in-plane vibration analysis of rectangular plates with elastically restrained edges. Journal of Sound and Vibration, 2007. 306(3-5): p. 908-927.
[37] Du, J.T., *et al.*, Free In-Plane Vibration Analysis of Rectangular Plates With Elastically Point-Supported Edges. Journal of Vibration and Acoustics-Transactions of the Asme, 2010. 132(3).
[38] Shi, D., *et al.*, A series solution for the in-plane vibration analysis of orthotropic rectangular plates with non-uniform elastic boundary constraints and internal line supports. Archive of Applied Mechanics, 2014: p. 1-23.
[39] Shi, X., *et al.*, A unified method for free vibration analysis of circular, annular and sector plates with arbitrary boundary conditions. Journal of Vibration and Control, 2014: p. 1077546314533580.
[40] Jin, G., *et al.*, An exact solution for the free vibration analysis of laminated composite cylindrical shells with general elastic boundary conditions. Composite Structures, 2013. 106(0): p. 114-127.
[41] Jin, G., *et al.*, A unified approach for the vibration analysis of moderately thick composite laminated cylindrical shells with arbitrary boundary conditions. International Journal of Mechanical Sciences, 2013. 75(0): p. 357-376.
[42] Chen, Y., G. Jin, and Z. Liu, Flexural and in-plane vibration analysis of elastically restrained thin rectangular plate with cutout

using Chebyshev–Lagrangian method. International Journal of Mechanical Sciences, 2014. 89(0): p. 264-278.

[43] Jin, G., *et al.*, A modified Fourier series solution for vibration analysis of truncated conical shells with general boundary conditions. Applied Acoustics, 2014. 85(0): p. 82-96.

[44] Jin, G., *et al.*, A general Fourier solution for the vibration analysis of composite laminated structure elements of revolution with general elastic restraints. Composite Structures, 2014. 109(0): p. 150-168.

[45] Wang, Q., *et al.*, Free vibration of four-parameter functionally graded moderately thick doubly-curved panels and shells of revolution with general boundary conditions. Applied Mathematical Modelling.

[46] Shi, D., *et al.*, A series solution for the in-plane vibration analysis of orthotropic rectangular plates with non-uniform elastic boundary constraints and internal line supports. Archive of Applied Mechanics, 2015. 85(1): p. 51-73.

[47] Shi, D., *et al.*, An accurate solution method for the vibration analysis of Timoshenko beams with general elastic supports. Proceedings of the Institution of Mechanical Engineers, Part C: Journal of Mechanical Engineering Science, 2015. 229(13): p. 2327-2340.

[48] Lv, X., *et al.*, 1953. A unified solution for the in-plane vibration analysis of multi-span curved Timoshenko beams with general elastic boundary and coupling conditions. Journal of Vibroengineering, 2016. 18(2).

[49] Shao, D., *et al.*, Transient response analysis of cross-ply composite laminated rectangular plates with general boundary restraints by the method of reverberation ray matrix. Composite Structures, 2016. 152: p. 168-182.

[50] Shao, D., *et al.*, A unified analysis for the transient response of composite laminated curved beam with arbitrary lamination schemes and general boundary restraints. Composite Structures, 2016. 154: p. 507-526.

[51] Shi, D., *et al.*, 2111. A unified solution for free vibration of orthotropic circular, annular and sector plates with general boundary conditions. Journal of Vibroengineering, 2016. 18(5).

[52] Shi, D., *et al.*, 1897. A unified solution for free vibration of orthotropic annular sector thin plates with general boundary conditions, internal radial line and circumferential arc supports. Journal of Vibroengineering, 2016. 18(1).

[53] Shi, D., *et al.*, A unified spectro-geometric-Ritz method for vibration analysis of open and closed shells with arbitrary boundary conditions. Shock and Vibration, 2016. 2016.

[54] Shi, X., *et al.*, A unified method for free vibration analysis of circular, annular and sector plates with arbitrary boundary conditions. Journal of Vibration and Control, 2016. 22(2): p. 442-456.

[55] Wang, Q., D. Shi, and Q. Liang, Free vibration analysis of axially loaded laminated composite beams with general boundary conditions by using a modified Fourier–Ritz approach. Journal of Composite Materials, 2016. 50(15): p. 2111-2135.

[56] Wang, Q., *et al.*, An improved Fourier series solution for the dynamic analysis of laminated composite annular, circular, and sector plate with general boundary conditions. Journal of Composite Materials, 2016. 50(30): p. 4199-4233.

[57] Wang, Q., *et al.*, A unified solution for free in-plane vibration of orthotropic circular, annular and sector plates with general boundary conditions. Applied Mathematical Modelling, 2016. 40(21): p. 9228-9253.

[58] Wang, Q., *et al.*, A unified solution for vibration analysis of moderately thick functionally graded rectangular plates with general boundary restraints and internal line supports. Mechanics of Advanced Materials and Structures, 2016(just-accepted): p. 00-00.

[59] Wang, Q., *et al.*, A unified solution for vibration analysis of functionally graded circular, annular and sector plates with general boundary conditions. Composites Part B: Engineering, 2016. 88: p. 264-294.

[60] Wang, Q., *et al.*, Vibrations of Composite Laminated Circular Panels and Shells of Revolution with General Elastic Boundary Conditions via Fourier-Ritz Method. Curved and Layered Structures, 2016. 3(1): p. 105-136.

[61] Wang, Q., D. Shi, and X. Shi, A modified solution for the free vibration analysis of moderately thick orthotropic rectangular plates with general boundary conditions, internal line supports and resting on elastic foundation. Meccanica, 2016. 51(8): p. 1985-2017.

[62] Shao, D., *et al.*, Free vibration of refined higher-order shear deformation composite laminated beams with general boundary conditions. Composites Part B: Engineering, 2017. 108: p. 75-90.

[63] Wang, Q., *et al.*, Benchmark solution for free vibration of thick open cylindrical shells on Pasternak foundation with general boundary conditions. Meccanica, 2017. 52(1): p. 457-482.

[64] Zhang, H., D. Shi, and Q. Wang, An improved Fourier series solution for free vibration analysis of the moderately thick laminated composite rectangular plate with non-uniform boundary conditions. International Journal of Mechanical Sciences, 2017. 121: p. 1-20.

[65] Wang, Q., *et al.*, Free vibration of four-parameter functionally graded moderately thick doubly-curved panels and shells of revolution with general boundary conditions. Applied Mathematical Modelling, 2017. 42: p. 705-734.

[66] Wang, Q., *et al.*, Free vibrations of composite laminated doubly-curved shells and panels of revolution with general elastic restraints. Applied Mathematical Modelling, 2017. 46: p. 227-262.

[67] Wang, Q., *et al.*, A unified formulation for free vibration of functionally graded carbon nanotube reinforced composite spherical panels and shells of revolution with general elastic restraints by means of the Rayleigh–Ritz method. Polymer Composites, 2017.

[68] Shao, D., *et al.*, An enhanced reverberation-ray matrix approach for transient response analysis of composite laminated shallow shells with general boundary conditions. Composite Structures, 2017. 162: p. 133-155.

Appendix A. Detailed expressions for the stiffness matrix and mass matrix

To make the expressions simple and clear, some indexes are pre-defined: s=(M+1)n+m+1, q=(M+1)$n1$+$m1$+1, s_1=(M+1)(l-1)+m+1, q_1=(M+1) (l-1)+$m1$+1, s_2=(N+1)(l-1)+n+1, q_2=(N+1) (l-1)+$n1$+1):

Sub-matrix $\mathbf{M}_{uu}$:

$$\left\{M_{uu}^{11}\right\}_{sq} = I_0 \int_0^R \int_0^\phi \left[\cos\lambda_{Rm} s \cos\lambda_{Rm1} s \cos\lambda_{\phi n}\theta \cos\lambda_{\phi n1}\theta\right](s+a)dsd\theta \tag{A.1}$$

$$\left\{M_{uu}^{12}\right\}_{sq_1} = I_0 \int_0^R \int_0^\phi \left[\cos\lambda_{Rm} s \cos\lambda_{Rm1} s \zeta_b^l(\theta) \cos\lambda_{\phi n1}\theta\right](s+a)dsd\theta \tag{A.2}$$

$$\left\{M_{uu}^{13}\right\}_{sq_2} = I_0 \int_0^R \int_0^\phi \left[\zeta_a^l(s) \cos\lambda_{Rm1} s \cos\lambda_{\phi n}\theta \cos\lambda_{\phi n1}\theta\right](s+a)dsd\theta \tag{A.3}$$

$$\left\{M_{uu}^{22}\right\}_{s_1q_1} = I_0 \int_0^R \int_0^\phi \left[\cos\lambda_{Rm} s \cos\lambda_{Rm1} s \zeta_b^l(\theta)\zeta_{b1}^l(\theta)\right](s+a)dsd\theta \tag{A.4}$$

$$\left\{M_{uu}^{23}\right\}_{s_1q_2} = I_0 \int_0^R \int_0^\phi \left[\zeta_a^l(s) \cos\lambda_{Rm1} s \cos\lambda_{\phi n}\theta\zeta_{b1}^l(\theta)\right](s+a)dsd\theta \tag{A.5}$$

$$\left\{M_{uu}^{33}\right\}_{s_2q_2} = I_0 \int_0^R \int_0^\phi \left[\zeta_a^l(s)\zeta_{a1}^l(s) \cos\lambda_{\phi n}\theta \cos\lambda_{\phi n1}\theta\right](s+a)dsd\theta \tag{A.6}$$

$$\left\{M_{uu}^{21}\right\} = \left\{M_{uu}^{12}\right\}^T; \left\{M_{uu}^{31}\right\} = \left\{M_{uu}^{13}\right\}^T; \left\{M_{uu}^{32}\right\} = \left\{M_{uu}^{23}\right\}^T; \tag{A.7}$$

Sub-matrix $\mathbf{K}_{uu}$:

$$\begin{aligned}\left\{K_{uu}^{11}\right\}_{sq} = {} & A_{11}\int_0^R\int_0^\phi \left[\lambda_{Rm}\lambda_{Rm1}\sin\lambda_{Rm}s\sin\lambda_{Rm1}s\cos\lambda_{\phi n}\theta\cos\lambda_{\phi n1}\theta\right](s+a)dsd\theta \\ & + A_{22}\int_0^R\int_0^\phi \left[\cos\lambda_{Rm}s\cos\lambda_{Rm1}s\cos\lambda_{\phi n}\theta\cos\lambda_{\phi n1}\theta/(s+a)\right]dsd\theta \\ & + A_{66}\int_0^R\int_0^\phi \left[\lambda_{\phi n}\lambda_{\phi n1}\cos\lambda_{Rm}s\cos\lambda_{Rm1}s\sin\lambda_{\phi n}\theta\sin\lambda_{\phi n1}\theta/(s+a)\right]dsd\theta \\ & + \left(ak_{r\_0}^u + bk_{r\_1}^u(-1)^{m+m1}\right)\int_0^\phi \cos\lambda_{\phi n}\theta\cos\lambda_{\phi n1}\theta d\theta \\ & + \left(k_{\deg\_0}^u + k_{\deg\_1}^u(-1)^{n+n1}\right)\int_0^R \cos\lambda_{Rm}s\cos\lambda_{Rm1}rd\theta\end{aligned} \tag{A.8}$$

$$\left\{K_{uu}^{12}\right\}_{sq_1} = A_{11}\int_0^R\int_0^\phi \left[\lambda_{Rm}\lambda_{Rm1}\sin\lambda_{Rm}s\sin\lambda_{Rm1}s\zeta_b^l(\theta)\cos\lambda_{\phi n1}\theta\right](s+a)dsd\theta \tag{A.9}$$
$$+A_{22}\int_0^R\int_0^\phi \left[\cos\lambda_{Rm}s\cos\lambda_{Rm1}s\zeta_b^l(\theta)\cos\lambda_{\phi n1}\theta/(s+a)\right]dsd\theta$$
$$+A_{66}\int_0^R\int_0^\phi \left[\lambda_{\phi n1}\cos\lambda_{Rm}s\cos\lambda_{Rm1}s\zeta_b^{l\prime}(\theta)\sin\lambda_{\phi n1}\theta/(s+a)\right]dsd\theta$$
$$+\left(ak_{r\_0}^u + bk_{r\_1}^u(-1)^{m+m1}\right)\int_0^\phi \zeta_b^l(\theta)\cos\lambda_{\phi n1}\theta d\theta$$

$$\left\{K_{uu}^{13}\right\}_{sq_2} = A_{11}\int_0^R\int_0^\phi \left[\lambda_{Rm1}\zeta_a^{l\prime}(s)\sin\lambda_{Rm1}s\cos\lambda_{\phi n}\theta\cos\lambda_{\phi n1}\theta\right](s+a)dsd\theta \tag{A.10}$$
$$+A_{22}\int_0^R\int_0^\phi \left[\zeta_a^l(s)\cos\lambda_{Rm1}s\cos\lambda_{\phi n}\theta\cos\lambda_{\phi n1}\theta/(s+a)\right]dsd\theta$$
$$+A_{66}\int_0^R\int_0^\phi \left[\lambda_{\phi n}\lambda_{\phi n1}\zeta_a^l(s)\cos\lambda_{Rm1}s\sin\lambda_{\phi n}\theta\sin\lambda_{\phi n1}\theta/(s+a)\right]dsd\theta$$
$$+\left(k_{\deg\_0}^u + k_{\deg\_1}^u(-1)^{n+n1}\right)\int_0^R \zeta_a^l(s)\cos\lambda_{Rm1}sd\theta$$

$$\left\{K_{uu}^{21}\right\}_{s_1q} = A_{11}\int_0^R\int_0^\phi \left[\lambda_{Rm}\lambda_{Rm1}\sin\lambda_{Rm}s\sin\lambda_{Rm1}s\cos\lambda_{\phi n}\theta\zeta_{b1}^l(\theta)\right](s+a)dsd\theta \tag{A.11}$$
$$+A_{22}\int_0^R\int_0^\phi \left[\cos\lambda_{Rm}s\cos\lambda_{Rm1}s\cos\lambda_{\phi n}\theta\zeta_{b1}^l(\theta)/(s+a)\right]dsd\theta$$
$$+A_{66}\int_0^R\int_0^\phi \left[\lambda_{\phi n}\cos\lambda_{Rm}s\cos\lambda_{Rm1}s\sin\lambda_{\phi n}\theta\zeta_{b1}^{l\prime}(\theta)/(s+a)\right]dsd\theta$$
$$+\left(ak_{r\_0}^u + bk_{r\_1}^u(-1)^{m+m1}\right)\int_0^\phi \cos\lambda_{\phi n}\theta\zeta_{b1}^l(\theta)d\theta$$

$$\left\{K_{uu}^{22}\right\}_{s_1q_1} = A_{11}\int_0^R\int_0^\phi \left[\lambda_{Rm}\lambda_{Rm1}\sin\lambda_{Rm}s\sin\lambda_{Rm1}s\zeta_b^l(\theta)\theta\zeta_{b1}^l(\theta)\right](s+a)dsd\theta \tag{A.12}$$
$$+A_{22}\int_0^R\int_0^\phi \left[\cos\lambda_{Rm}s\cos\lambda_{Rm1}s\zeta_b^l(\theta)\theta\zeta_{b1}^l(\theta)/(s+a)\right]dsd\theta$$
$$+A_{66}\int_0^R\int_0^\phi \left[\cos\lambda_{Rm}s\cos\lambda_{Rm1}s\zeta_b^{l\prime}(\theta)\zeta_{b1}^{l\prime}(\theta)/(s+a)\right]dsd\theta$$

$$+\left(ak_{r\_0}^{u}+bk_{r\_1}^{u}(-1)^{m+m1}\right)\int_0^{\phi}\zeta_b^l(\theta)\zeta_{b1}^l(\theta)d\theta$$

$$\left\{K_{uu}^{23}\right\}_{s_1q_2}=A_{11}\int_0^R\int_0^{\phi}\left[\lambda_{Rm1}\zeta_a^{l\prime}(s)\sin\lambda_{Rm1}s\cos\lambda_{\phi n}\theta\zeta_{b1}^l(\theta)\right](s+a)dsd\theta \tag{A.13}$$
$$+A_{22}\int_0^R\int_0^{\phi}\left[\zeta_a^l(s)\cos\lambda_{Rm1}s\cos\lambda_{\phi n}\theta\zeta_{b1}^l(\theta)/(s+a)\right]dsd\theta$$
$$+A_{66}\int_0^R\int_0^{\phi}\left[\lambda_{\phi n}\zeta_a^l(s)\cos\lambda_{Rm1}s\sin\lambda_{\phi n}\theta\zeta_{b1}^{l\prime}(\theta)/(s+a)\right]dsd\theta$$

$$\left\{K_{uu}^{31}\right\}_{s_2q}=A_{11}\int_0^R\int_0^{\phi}\left[\lambda_{Rm}\sin\lambda_{Rm}s\zeta_{a1}^{l\prime}(s)\cos\lambda_{\phi n}\theta\cos\lambda_{\phi n1}\theta\right](s+a)dsd\theta \tag{A.14}$$
$$+A_{22}\int_0^R\int_0^{\phi}\left[\cos\lambda_{Rm}s\zeta_{a1}^l(s)\cos\lambda_{\phi n}\theta\cos\lambda_{\phi n1}\theta/(s+a)\right]dsd\theta$$
$$+A_{66}\int_0^R\int_0^{\phi}\left[\lambda_{\phi n}\lambda_{\phi n1}\cos\lambda_{Rm}s\zeta_{a1}^l(s)\sin\lambda_{\phi n}\theta\sin\lambda_{\phi n1}\theta/(s+a)\right]dsd\theta$$
$$+\left(k_{\deg\_0}^{u}+k_{\deg\_1}^{u}(-1)^{n+n1}\right)\int_0^R\cos\lambda_{Rm}s\zeta_{a1}^l(s)d\theta$$

$$\left\{K_{uu}^{32}\right\}_{s_2q_1}=A_{11}\int_0^R\int_0^{\phi}\left[\lambda_{Rm}\sin\lambda_{Rm}s\zeta_{a1}^{l\prime}(s)\zeta_b^l(\theta)\cos\lambda_{\phi n1}\theta\right](s+a)dsd\theta \tag{A.15}$$
$$+A_{22}\int_0^R\int_0^{\phi}\left[\cos\lambda_{Rm}s\zeta_{a1}^l(s)\zeta_b^l(\theta)\cos\lambda_{\phi n1}\theta/(s+a)\right]dsd\theta$$
$$+A_{66}\int_0^R\int_0^{\phi}\left[\lambda_{\phi n}\lambda_{\phi n1}\cos\lambda_{Rm}s\zeta_{a1}^l(s)\zeta_b^{l\prime}(\theta)\sin\lambda_{\phi n1}\theta/(s+a)\right]dsd\theta$$

$$\left\{K_{uu}^{33}\right\}_{s_2q_2}=A_{11}\int_0^R\int_0^{\phi}\left[\zeta_a^{l\prime}(s)\zeta_{a1}^{l\prime}(s)\cos\lambda_{\phi n}\theta\cos\lambda_{\phi n1}\theta\right](s+a)dsd\theta \tag{A.16}$$
$$+A_{22}\int_0^R\int_0^{\phi}\left[\zeta_a^l(s)\zeta_{a1}^l(s)\cos\lambda_{\phi n}\theta\cos\lambda_{\phi n1}\theta/(s+a)\right]dsd\theta$$
$$+A_{66}\int_0^R\int_0^{\phi}\left[\lambda_{\phi n}\lambda_{\phi n1}\zeta_a^l(s)\zeta_{a1}^l(s)\sin\lambda_{\phi n}\theta\sin\lambda_{\phi n1}\theta/(s+a)\right]dsd\theta$$
$$+\left(k_{\deg\_0}^{u}+k_{\deg\_1}^{u}(-1)^{n+n1}\right)\int_0^R\cos\lambda_{Rm}s\zeta_{a1}^l(s)d\theta$$